ADDIS ABABA UNIVERSITY

ADDIS ABABA INSTITUTE OF TECHNOLOGY

SCHOOL OF CIVIL AND ENVIRONMENTAL ENGINEERING

FLOOD RISK ASSESSMENT USING MULTI-CRITERIA EVALUATION AND FLOOD INUNDATION MODELLING: THE CASE OF UPPER AWASH BASIN, ETHIOPIA

By:

Reta Birhanu

GSR/4239/10

Advisor:

Dr. Ermias Teferi

A Thesis submitted to

School of Graduate Studies of Addis Ababa University in Partial fulfillment of the requirements for the Degree of Masters of Science in Geodesy and Geomatics

(Specialization in Geomatics)

Addis Ababa 2020

Addis Ababa University

Addis Ababa Institute of Technology (AAiT)

School of Civil and Environmental Engineering

This is to certify the Thesis Prepared by Reta Birhanu, entitled as 'Flood Risk assessment using multi-criteria evaluation and flood inundation modelling: the case of Upper Awash basin, Ethiopia' Is Submitted in Partial Fulfillment of the Requirements for The Degree of Master of Science in Geodesy and Geomatics (Specialization in Geomatics) Compiles with the Regulations of the University and Meets the Accepted Standards with its Originality and Quality.

Approved by board of examiners:

Dr. Ermias Teferi

Advisor ______________________ Signature ______________ Date

Dr. Worku Zewdie

Internal Examiner ______________________ Signature ______________ Date

Dr. Berhan Gessese

External Examiner ______________________ Signature ______________ Date

____

Chair person ______________________ Signature ______________ Date

Declaration

I hereby declare that this thesis, entitled "Flood Risk assessment using multi-criteria evaluation and flood inundation modelling: the case of Upper Awash basin, Ethiopia" which I submit to School of Civil and Environmental Engineering of Addis Ababa University Institute of Technology in partial fulfillment of the requirement of degree of Master of Science in Geodesy and Geomatics (Specialization in Geomatics), is my original work carried out under the supervision of Ermias Teferi (PhD). It has not been presented for a degree in any other universities and all sources of materials used for the thesis work have been properly acknowledged.

Reta Birhanu Endale	____________________	____________
Student Name	Signature	ID

This MSc Thesis has been submitted for Examination with My Approval as Thesis advisor.

Dr. Ermias Teferi	____________________	____________
Advisor Name	Signature	ID

ACKNOWLEDGMENTS

First and for most, I would like to thank Jesus for his provisions, protections and support in my entire life and the holy mother Saint Mary.

This thesis would not have been possible without the help and guidance of several individual who in one way or another contributed and extended their valuable assistance in preparation and completion of this study. In fact it is impossible to list all of the, therefore the following list is horribly incomplete. However it would be worse not to make an attempt to acknowledge those who have played a key role in my work.

My deeper gratitude goes to my advisor, Dr. Ermias Teferi who patiently corrected the manuscript and provided me valuable comments and also for his kind guidance, providing different solution and motivation towards my master thesis.

I remain indebted to the Addis Ababa university community in general and the Department of Geodesy and Geomatics staff in particular for their cooperation during my stay in this campus.

I am grateful to all Ministry of water, irrigation and energy staff, Central statistics Agency, Ethiopian Mapping Agency (Geospatial Information Institute) staffs for unforgettable cooperation in during my data collection work to achieve my objective.

.

Finally I would like to thank my family, relatives, friends and others who helped me and contributed helpful advice in accomplishing my thesis work.

Table of Contents

List of Tables

List of Figures

List of Abbreviations

AHP: Analytic Hierarchy Process

ASTER: Advanced Space borne Thermal Emission and Reflection Radiometer

CSA: Central Statistics Agency

DEM: Digital Elevation Model

DPPA: Disaster Preparedness and Prevention Agency

DTM**:** Digital Terrain Model

FCC: False Color Composite

FFA: Flood Frequency Analysis

GIS: Geographical Information System

GPS: Global Positioning System

HEC-RAS: Hydrologic Engineering Center River Analysis System

ITCZ: Inter Tropical Convergence Zone

MCA: Multi Criteria Analysis

NMA: National Meteorological Agency

OCHA: Office for the Coordination of Humanitarian Affairs

OLI: Operational Land Imager

SAR: Synthetic Aperture Radar

TIN: Triangulated Irregular Network

TM: Thermal Mapper

UN: United Nation

WRDA: Water Resources Development Authority

WWDSE: Water Works Design and Supervision Enterprise

ABSTRACT

Flood is among the most common widely recognized and destructive natural hazards causing extensive damage to infrastructure, public and private services, the Environment, the economy and devastation to human settlements. The objective of this thesis is Evaluation of flood hazard and risk prone sites: the case of upper awash basin. To achieve the objective flood assessment is performed using a Multi Criteria Analysis (MCA) in a GIS environment. To produce the flood hazard seven flood causative factors were considered, these are the reclassified, Elevation, Rainfall intensity (precipitation), Drainage Density, Elevation, Slope, Distance to River, soil type and Land use/cover map of the study area. The result has revealed that, 9.18 % of the basin was characterized by very high flood hazard level and 36.08 % of the study area was characterized by high flood hazard level. On the other hand 45.14 % of the study area fall under moderate hazard level zone. The rest of the study area which is 9.46 % and 0.14 % falls under low and very low hazard level respectively. Flood risk assessment was done by taking the population and land use land cover as element at risk. Unlike the flood hazard analysis the result of flood risk analysis shows that 4.43, 15.73, 41.35, 28.82 and 9.67 percent of the area of the upper awash basin were subjected to very low, low, moderate, high and very high flood risk respectively. For flood inundation modelling Log Normal distribution, Gumbel’s distribution and Log Pearson distributions were compared to choose best distribution for estimation of discharge at the return period of 5, 10, 25, 50, 100, and 200 year, however flood extent map were prepared for the return period of 50, 100 and 200 year. From the result of 50 year return period inundation modelling it is observed that most flood depths are in range of 0.00-0.52m which covers 27% of the total flood extent. The next highest portion is covered by 0.52-0.91m which is about 22%. Other flood depths 0.91m-1.60m, 1.60-2.47m and 2.47-3.67m takes in decreasing proportion.

CHAPTER ONE

INTRODUCTION

1.1 Background

Flood issue has been reported almost everywhere on the world with considerably more articulated impacts in the poor countries because of their low income, poor housing facilities, lack of proper warning system and preparedness, in general these are grouped into financial, political and social weaknesses Alcantara (2002). Floods are related with two sort of impacts the first is impacts like loss of lives and property, damage to infrastructure, eco-system, cultural values, roads and bridges which are considered as an primary impact Jonkman (2005), on the other hand effects such as outbreak of diseases is known as secondary effect, as well as tertiary effects like loss of soil fertility, famine and poverty.

Large and damaging floods happened in numerous country of the world, some of these are Heavy floods that occurred in Pakistan, India and China in the summer of 2010, Colombia from October to December 2010 and Australia during the austral summer 2010/11. The most extreme assessed yearly damage brought about by river floods in a single nation was recorded in China in 2010, where an all-out loss of US$51 billion was accounted for. In 2010, there were about 2000 immediate fatalities from monsoonal flooding in Pakistan Syvitski et al. (2013).

In the last three decades, there has been an ascent in flooding events all around the world. A recent report by the Belgian-put together Center for research with respect to Epidemiology of debacles (CRED) and UN Office for Disaster Risk Reduction UNISDR (2015) on "The human cost of climate related fatalities" revealed that the death occurring from flooding has risen universally. It further revealed between 1995 and 2015, a total of 2.3 billion individuals were influenced by floods around the world. The report shows that flood related hazard is significantly higher than other kind of climate related hazard. Additionally, the figure of the report indicates that Asia and Africa are the most affected by flood as compared to other continents but pose an increasing danger elsewhere.

As per the report of the report of United Nations Office for the Coordination of Humanitarian Affairs OCHA (2019) showed that Ethiopia was encountering flooding in numerous parts the country. The figure shows that a sum of 202,202 individuals have been displaced across the nation, the dominant part (127,524 individuals) in Somali region. More than 17,000 family units were displaced in Shabelle zone of the Somali region. Over 17,000 households were displaced in Shabelle zone of the Somali region. Latrines, schools buildings and health facilities have been damaged or destroyed. Meanwhile in Dollo Ado woreda (district), over 3,500 families have been displaced. Roads have been blocked and livestock and crops have been damaged or destroyed. According to the report landslide killed 22 people in Konta special woreda (Amaya town). UN-OCHA said that floods and landslides were also reported in Melokoza woreda of Gofa zone and Zabageze woreda of Dawuro zone. This report also showed that In Afar Region the Awash River broke its banks earlier this month, damaging or destroying 4,250 homes and affecting over 7,000 families.

In Amhara district in OCHA (2006) extreme flooding influences and displaced 43,127 and 8,728 people groups individually. On 5 August 2006, heavy rains made the Dechatu River burst its banks, causing serious flash flooding in the regions of Dire Dawa. Disaster Preparedness and Prevention Agency (DPPA) confirmed that floods in South Omo Valley killed 364 people and displaced approximately 6000 – 10,000 more following heavy rains which forced the Omo River to burst its banks and flood five villages in remote southern Ethiopia.

Heavy rains across the country have seen further flooding in South Omo Valley, Dire Dawa, Amhara, Afar, Somali, Tigray, Gambella and Oromiya regions. Report from government and United Nations (UN) demonstrated that, around 35,000 individuals have been dislodged, 120,000 influenced and 620 confirmed dead. These report does not take into account population group who were temporarily located to the higher ground.

1.2 Statement of Problem

The surrounding area of upper awash basin is subjected to different events of river floods in summer time especially from June to September due to over flow of Rivers. These river floods are among the most frequent and exorbitant catastrophic events by causing devastation of scant rural land on the study area and demolition of are lost in the in the study area every year and most part of Illu woreda especially becho plain, Ejere woreda, sebeta awas woreda around Atebela and some part of Akaki Kaliti sub-city are subjected to flooding problems every year during the rainy season and the flood causes loss of human life and property damage in this woredas.

Awash River is one of the rivers which cause flooding at Becho, Illu, Sebeta and Ejerie floodplain. The river conveys high runoff from upper catchments and local rainfall on the floodplain by resulting in flooding problems in the surrounding area. The Joint Government and Humanitarian Partners, in 2006 reported that about 4,506 hectare of different crops have been damaged and livestock disease outbreaks are anticipated by floods as it is located at lower level in the river on Illu-Sebeta and Ejerie floodplains. On the other hand Akaki River is also one of the River in Upper Awash Basin causing flooding problem Around Akaki kaliti and its surrounding area during the rainy season.

Different flood related analysis has been carried out in the upper awash basin, however Most of this studies are restricted to some part of the Upper awash basin. Some of these are (Dawit, 2015) carried out his flood risk analysis on Illu flood plain and (Abebe, 2007) tried to address of flood hazard assessment in becho plain, both of these studies are limited to a specific area of the Upper Awash Basin. This situation requires appropriate flood risk assessment. To do this Remote sensing (RS) and geographic information system (GIS) techniques have made significant contributions.

1.3 Objectives

1.3.1 General Objectives

The main objective of this study is to develop the flood risk map and to model flood inundation in the case of Upper Awash River Basin.

1.3.2 Specific Objectives

The specific objective of this thesis were:

- ✓ To develop flood hazard map of the Upper Awash River Basin
- ✓ To develop flood risk map of the upper awash basin
- ✓ To model flood inundation in upper awash River basin.
- ✓ To determine best distribution for prediction of discharges for different return period

CHAPTER TWO

LITERATURE REVIEW

2.1 Flood characterization

Flood is among the most common and destructive natural hazards known by its extensive damage to infrastructure, public and private services, the Environment, the economy and destruction to residential area. Floods stand out to be the most frequent and devastating natural disaster around the world Sanyal et al. (2006), affecting a millions people every year.

Types of floods: Generally, classification of floods can be done by establishing the main difference between flood types. This is done by considering factors like the size of the affected area and the time taken by the driving precipitation event. These two elements are then useful in defining the spatial and temporal scale of flood events consequently leading to two main classes of extensive long lasting floods and local sudden floods Bronstert (2003). A number of literatures classified Flood types into three main types namely; river flood, flash flood and storm surge Perry et al. (2000). Perry et al. (2000) further categorizes floods as ice-jam floods, dam-and levee-failure floods debris, landslide and mudflow floods but emphasizes that these types are rather less common.

Knowledge of flood type is important for proper planning; flood monitoring, management and development of flood early warning systems as well as assessment of flood damage (Huang, 2008).

Most common flood types reported in literature are briefly described and include the following;

Coastal floods: this is a type of floods that occur along the coasts of the seas and big lakes. The triggering factor for this type of floods are wind storms such as cyclones and low atmospheric pressure that eventually result to the set-up of water levels on the coast Berzet et al. (2001). It is mentioned that when this set-up of water levels coincides with astronomical high tide at the coast, coastal floods can lead to high water levels and thus flooding of the coastal area Jonkman (2005).

Flash floods: this type of flood occur as a result of a heavy and intensity localized rainfall and it is known by its sudden occurrence and quick raise of water which is a threat to life and property.

Younis et al. (2008). Other factors that are known to have contribution on this kind of floods are steep slopes, impervious ground surfaces and low permeability soils Younis et al. (2008). The prediction and cautioning becomes troublesome in light of the abrupt event of flash floods by leaving very brief timeframe. Moreover the high increasing rate and flow velocity of flash floods likewise make them more dangerous to human lives than river floods Younis et al. (2008). Property damage and Death caused by flash flood are more articulated when contrasted with other type of floods (jonkman, 2005).

River floods: refers to a flood type caused as a result of flooding of the river outside its regular boundaries. They can likewise be related by a break of barriers or dams close to the river. As per Jonkman (2005), river floods can be caused by various sources including high precipitation levels, melting snow and blockage of the flow. Unlike flash floods, river floods can be predicted in some period in advance Jonkman (2005).

2.1.1 Flood Risk Concept

An attempt by the risk experts in late1970's to come up with the standard definition of risk concluded that a common definition is perhaps unachievable, and authors should continue to define the risk in their own way. As a result, a number of definitions for risk can be found from fuzzy and conceptual to rigid and quantitative. At conceptual level risk can be defined in three ways, first a significant potential unwelcome effect of system performance, or second the predicted or expected likelihood that a set of circumstances over some time frame will produce some harm that matters, or third future issues that can be avoided or mitigated, rather than present problems that must be immediately addressed Simonovic (2009). Singh (2007) classified risk into three categories: (i) risk for which statistics of the identified causalities are available; (ii) risk for which there may be some evidences, but where the connection between suspected cause and damage cannot be established; and (iii) estimates of the probabilities of the events that have not been occurred. Additionally, there are risks that are unforeseen.

(a) Hazard: can be defined as the probability that in a given period in a given area, extreme potentially damaging natural event occurs that induce air, earth movements, which influence a specific region. The size of the event, the likelihood of its occurrence and the degree of its effect can change and can be resolved.

(b) **Vulnerability:** is characterized as any physical, structural, or socio-economic element to a natural hazard is its likelihood of being damaged, destroyed or lost. Vulnerability is considered as a dynamic process, incorporating changes and developments that alter and influence the likelihood of loss and damage of all exposed elements. Vulnerability can also be defined as the measure of the capacity to weather, resist, or recover from the impacts of a hazard in the long term as well as the short term. Vulnerability relies on numerous variables, for example, land use, extent and type of construction, contents and use, the nature of populations (mobility, age, health), and warning of an impending hazardous event and willingness and capacity to take responsive activities. Vulnerability to flood incorporates the blend of four distinctive types of vulnerabilities: physical, economic, infrastructure and social.

I. Physical vulnerability: generally incorporates only those indicators susceptible to biological sensitivity. Wetlands are for example, considered regions of physical vulnerability. Wetlands are among the most productive ecosystems on earth. The richness of these transitional ecosystems relates mostly to the diversity of ecological niches created by the variability of seasonal and inter–annual cycles. Modifications in the hydrologic regime that disturb these cycles have been found to be the main stress factor threatening shoreline wetlands in all the world's major rivers . The regulation of water levels has also caused the shrinkage of wetlands, and an incidental reduction in the diversity of plant communities and the number of plant species .These regions have high biodiversity and sensitive life, which would experience higher damages, longer, slower recovery times due to flooding.

II. Economic vulnerability: includes flood damage indicators which can be expressed in monetary terms.

III. Infrastructure vulnerability: this includes civil structure such as road networks, railways, and road bridges considered as physical vulnerability. Infrastructure components are important to movement of population, communications, and safety. Their inundation impedes traffic and hinders communications, increasing stress in the exposed population. Inundation may also block important emergency routes and cause physical damage to roads.

IV. Social vulnerability: focuses on the reaction, response, and resistance of a population to a disastrous event. Vulnerable population may require special attention in an evacuation situation for example Karmakar (2010).

Risk can be related directly to the concept of disaster, given that it includes the total losses and damages that can be suffered after a natural hazard: death and injured people, damage to property and interruption of activities. Risk implies a future potential condition, a function of the magnitude of the natural hazard and of the vulnerability of all the exposed elements in a determined moment. Risk is a factor, element, or course involving danger or can be seen as the possibility of suffering harm or loss (Encarta, 99).It can also be mathematically calculated as the product of hazard, exposure, and vulnerability. By following this approach a large GIS database can be designed and developed in order to spatially represent the three components of risk. Flood risk may be described at different scales, ranging from the global to the local scale. Risk has become an issue that is being discussed in various fields where in varied definitions have been given Stig (1996). Studies of risk cover the issues such as identification and estimation of risk, risk assessment and evaluation, including monitoring and management of risk Gerrard (1995).

2.2 Flood frequency Analysis

Hydrologic systems are sometimes impacted by extreme events, such as severe storms, floods, and droughts. The magnitude of an extreme event is inversely related to its frequency of occurrence, very severe events occurring less frequently than more moderate events, Chow (1998).

The objective of frequency analysis of hydrologic data is to relate the magnitude of extreme events to their frequency of occurrence through the use of probability distributions Dawit (20015).

The results of flood flow frequency analysis can be used for many engineering purposes: such as for the design of dams, bridges, culverts, and flood control structures; to determine the economic value of flood control projects; and to delineate flood plains and determine the effect of encroachments on the flood, Dawit (2015)

According to Chow (1998), there are a number of distributions in hydrology used to analyze the probability of occurrence of a stream flow. Some of these are Normal distribution, lognormal distribution, Pearson type III distribution, Log-Pearson type III distribution, Exponential distribution, Extreme value distribution and Gamma distribution.

2.3 Methods of risk assessment

2.3.1 Hydraulic and hydrologic method

Karagiozi (2011) assessed flood risk by employing hydrological model into Geographic Information System (GIS) environment (Arc hydro Model) by taking in to account the geomorphological characteristic of the study area. According to this study flood hazard factors were combined by using simple multiplication in order to produce the flood hazard map for each water basin and enhance the spatial differentiation of the phenomena. The resulting flood hazard map was published into a web GIS environment providing a friendly Graphic User Interphase (GUI) to the end users that can interact dynamically with the map.

Emanual et al. (2015) performed flood risk assessment with application of Remote Sensing and Geographic Information system for flood risk management in Dhaka town. In their study they employed satellite 5, for Landsat 7 L1T images and ASTER L1A images. The study focuses on the assessment of urban expansion and the flood hazard occurring in the study area.

The study compares classification of the Landsat images through the change detection analysis to quantify land use/ land cover changes and systematically flooded area. In this study Landsat images of built up areas from 2000, 2002, and 2009 were assembled and highlighted the urban expansion of the study area. The study was performed by processing eight Landsat image and the ASTER multispectral images to quantify urban expansion and investigation of flooding evolution by using post classification comparison.

Flood hazard mapping and risk assessment of Bagmati river in central Nepal was done to identify the priority areas and high risk zones using Advanced Spaceborne Thermal Emission and Reflection (ASTER) image combined with hydraulic model (HEC–RAS) which was used to simulate flood flows through the river and its flood plain for discharges corresponding to various return periods using annual maximum instantaneous discharges for the period from 1965–2004. The model results were verified through a field visit and data collected on flood depths corresponding to the peak flood of year 2004 that had a magnitude close to that of a 50year flood. Vulnerability was assessed based on the economic importance of land type being inundated and population density using Census Data (2001) from Central Bureau of Statistics, Nepal. Finally flood risk factor was determined using the flood hazard and vulnerability factors based on matrix multiplication method on VDC level Kafle (2006).

Ologunorisa (2004) carried out flood risk assessment in the Niger Delta, Nigeria using a combination of hydrological techniques based on some measurable physical characteristics (depth of flooding (m), duration of flood (hrs/weeks), perceived frequency of flood occurrence, and relief or elevation (m) of flooding, and social-economic techniques based on vulnerability factors (proximity to hazard source, land use or dominant economic activity and adequacy of flood alleviation schemes and perceived extent of flood damage). 18 settlements were randomly selected across the three ecological zones in the region were rated on the basis of the said parameters using rating scale. Three flood risk zones emerged from the analysis and these are the severe flood risk zones, moderate flood risk zones and low flood risk zones.

2.3.2 Remote Sensing and GIS approach

Forkuo (2011), has generated efficient and cost effective methodology for preparing flood hazard maps in Ghana, particularly those regions where floods pose a recurrent danger. The level 1b ASTER imagery, topographic map covering the study area at a scale of 1:50000, the contours generated DEM, land cover and demographic data has been used to create a district level map indicating flood hazard index for district scale using an additive model which was adapted for this study Sanyal et al. (2003).The hazard categories of classification was based on the Jenks scheme (natural break).

Fosu (2012), has illustrated the case study of the Susan River, Ghana. He employed the land cover data obtained from classified ASTER image, the contour generated DEM, the geometric data extracted from the DEM, topographic map and field measurements collections. HEC-RAS model (i.e., open channel flow) used as main model to calculate floodplain elevations and determine floodway encroachments. the geometric data coalesced with the topographic maps to generate the flood hazard maps that covers an approximately 2.93 km² indicating flood depth of 4.02 m was obtained as the maximum water level and high water depth occurred along the main channel and spreads gradually to the floodplains. The recent satellite images of high resolution With the little data availability (e.g. cadastral, topographical, hydrological, and meteorological Guarin et al. (2004) perform the basic flood risk assessment by combining aerial photo interpretation, the use of data questionnaires in a community-based field data collection, and subsequent analysis using Geographical Information Systems (GIS) in study area of San Sebastian based on traditional hydrological modeling. The cadastral base map with an attribute database was generated as key inputs for flood hazard and vulnerability assessment of the area. The vulnerability maps were combined with the cost information for the estimation of the loss. The flood vulnerability curves relating water height and speed were assessed for the three of the main elements at risk within the urban area: buildings, contents, and road network. The municipal authorities used the generated cadastral map with database containing physical and social information at the parcel level as well as detailed information on flood hazard, vulnerability and expected losses, as a valuable tool in municipal planning, including a wider range of applications in addition to risk management.

2.4 Flood Disaster Management

In the management of flood disasters, flood hazard/risk mapping is one of the vital steps undertaken to prepare for and mitigate the effects of a flooding event. Some of the other vital steps may include vulnerability analysis, climate forecasting, flood plain management and enforcement of standards and codes. Weston (2000) and United Nations (2012.)

2.4.1 Vulnerability Analysis

The population and structures within areas delineated as flood-prone are looked at during a vulnerability analysis. During the vulnerability analysis, the potential costs of flooding are evaluated as pertaining to damage of critical infrastructure such as utilities, bridges roads, buildings and crops. Because vulnerability analysis detects the population at utmost risk, it can also be used to determine the emergency responses that may be essential such as temporary shelters and evacuation parameters. United Nations (2012)

2.4.2 Climate Change Forecasting

Based on identified changes in the patterns of ocean and atmospheric circulation, the magnitude of a storm can be forecasted and this information can help in emergency response preparedness. This information can be used to reduce the severity of flooding when it occurs by creating awareness, increasing food storage and management of fresh water, Doornkamp (1998)

2.4.3 Flood Plain Management

Activities within areas identified as flood prone can be managed so as to minimize flood damage to existing infrastructure. The measures undertaken to manage activities can be grouped into two; structural and nonstructural measures. Structural measures deals with the construction of protective works such as flood storage reservoirs, storm channels and embankments to carry water away from the flood area. Nonstructural measures help in controlling development in flood prone areas at a low cost. Land-use planning, Zoning of flood-prone lands, Redevelopment of flood-prone areas, Compensation, incentives and Insurance are some of the nonstructural measures that can applied. Stewart (2002).

2.4.4 Enforcement of Standard and Codes

Standards and codes for flood-prone areas should be enforced to help minimize the impact of flood events. Enforcement procedures should be simple enough to aid the implementation of penalties with regards to noncompliance to the standards and codes. Regular emergency response drills should be undertaken to ensure that flood prevention measures still work. United Nations (2012).

2.5 Flood scenario in Ethiopia

In Ethiopia flooding usually occurs within the three months of the rainy season and limited to areas of lower and flat topographic setting. It is usually the intense rainfall in the high lands that cause flooding at its downstream and disaster to settlements close to any stretch of river courses Isaak (2002).

Moreover, flood hazard is common to the floodplains which are normally located along the rivers at the downstream parts of the river courses. The Awash River Basin is one of the five main basins which has encountered wide floodplains along its courses. At its middle and lower catchments there are known flood events once every year during the rainy season of summer. In the lower catchments the hazardous flood to agriculture and settlement is caused by the over flow of river Mille and Logiya which are main tributaries of the Awash River. In its middle catchment, Kessem and Kebena are other tributaries of Awash River that cause main flooding.

Moreover, there are also other basins where there are high flood hazards to property and humans living within the floodplains. Those basins that cause major flood problem in the country are the lower part of Wabishebelle, Baro-Akobo, and Omo Basins.

During flood occurrence in Dire Dawa during in August 1981 80 people were killed , and the other unpredicted flood that occurred on August 6, 2006 flooding was worst of all flooding event in Dire Dawa that killed 256 people from which 244 were missed and 15,000 people were displaced.

In 2006 a total of 524,400 people were vulnerable to flood disaster throughout the country during the rainy season of Ethiopia. Out of this population, 199,900 people are actually affected by flood disaster in various regions of the country Assefa (2011).

For conducting this thesis the Remote Sensing and GIS based approach was used for flood risk assessment and flood inundation modelling was performed using HEC-RAS/HEC-Geo-RAS software because this method can be employed with the data at hand. The method is also feasible in terms of time as well as in terms cost.

CHAPTER THREE

MATERIAL AND METHODS

3.1 Study Area

The Awash River Basin in Ethiopia is located on a geographic between $8^{o}5'$and $12\ ^{o}$ N and approximately 38^{o} and 42^{o}E. The river basin at an elevation of 3000msl from 150km west of Addis Ababa. The total land area covered by this basin is of 110,000 km^2, from this 64 000 km^2 of the land area is included under the Western Catchment, drains to the main river or its tributaries. The remaining 46 000 km^2, most of which comprises the so called Eastern Catchment, drains into a desert area and does not contribute to the main river course.

The Awash Basin is traditionally divided into four distinct zones. These are; Upper Basin, Upper Valley, Middle Valley and Lower Valley.

Table 1 Awash Basin Division

Designation	From	To
Upper Basin	Headwaters	Koka Dam
Upper Valley	Koka Dam	Awash Station
Middle Valley	Awash Station	Gewane
Lower Valley	Gewane	Lake Abe

Source: Shimelis, 2004

The river ascends from the Mountainous area near Ginchi town west of Addis Ababa in Ethiopia and streams along the rift valley into the Afar triangle, and ends in salty Lake Abbe on the border with Djibouti, being an endorheic basin. The all out length of the main course is nearly 1,200 km.

Upper Awash River Basin is located in the central Ethiopia in oromia regional state. The location of the study area is in Upper Valley from Headwaters up to Koka Dam (3,000-1600 meters elevation). The Total Area of this catchment is estimated to be 11,228 square km. The basin is delimited on its western side by the Abbay River basin, to the south-west by the Omo-Gibe and Rift Valley Lakes Basin and to the south-east by the Wabi Shebele River Basin. The Upper Awash

River Basins contains sub-basins like hombole sub-basin, Mojo sub-basin, Melka Kuntire sub-basin, Akaki Subbasin, Bello Sub-basin and Teji sub-basins.

The Awash River and several feeders ascends from these mountains that reach over 3300 m.a.s.l. The Berga, Holeta, Kelina, Dilolo Dilu, Teji and Watira tributaries join the Awash River in the Becho plain that flows towards Lake Koka in southeastern direction. The catchment of this upstream part of the upper awash reach until the gauging station at Melka Kunture is 4541 km^2 according to Ethiopian Valleys Development Studies Authority EVDSA (1989).

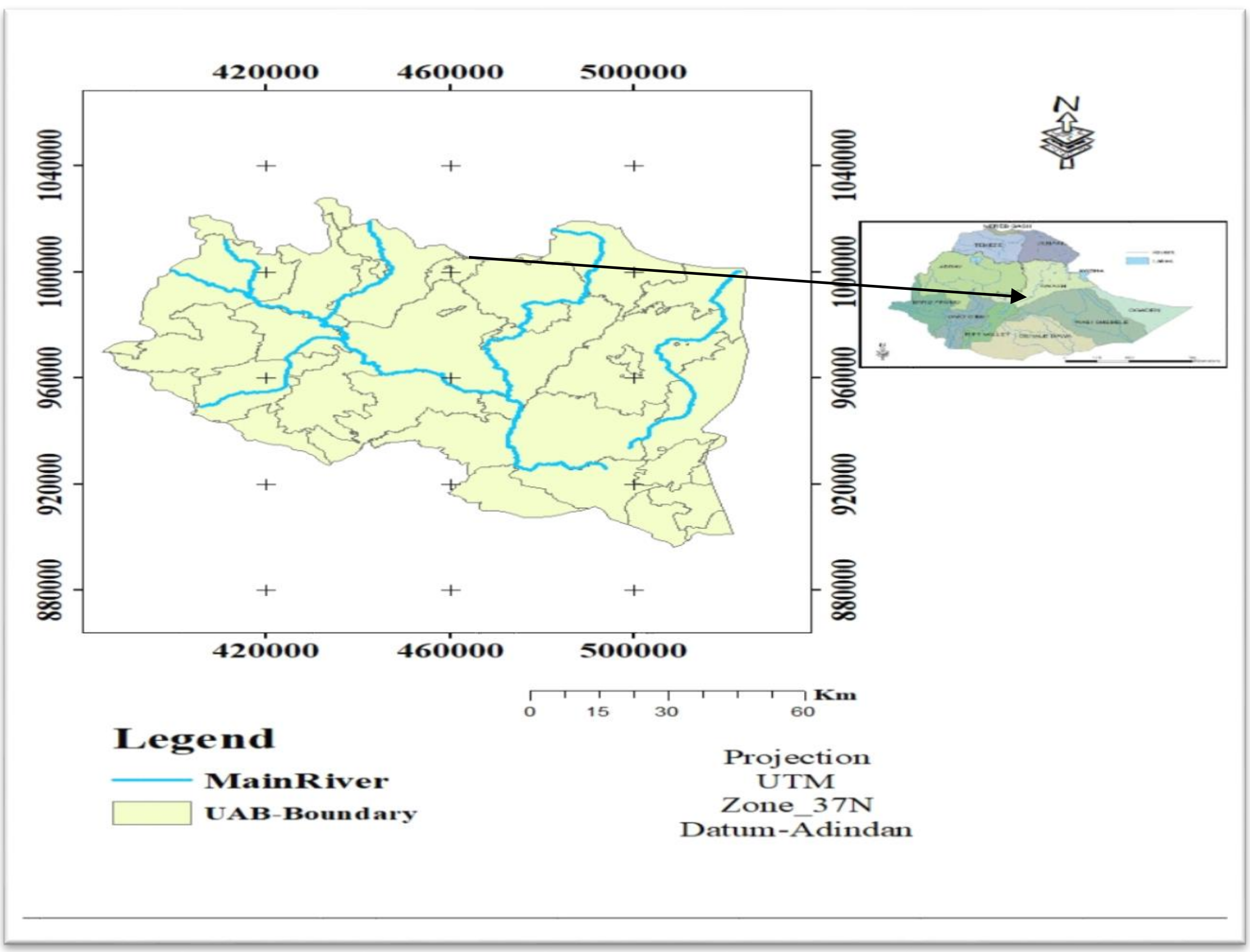

Figure 1 Map Study Area

3.1.2 Climate in the study area

The climate of this Ethiopia part is dominated by the movement of the Inter Tropical Convergence Zone (ITCZ) that permits dry easterlies or moist westerly. In March the ITCZ progresses over the Awash Basin acquiring spring rains in the 'Belg' season. The ITZC reaches its most northern position when heavy summer rains come from the west. This season is the main rainy season called 'Kiremt' and lasts until September. Than the dry months of the dry season called 'Bega' extend from October to February EVDSA (1989). The measure of precipitation is affected by orographic highlights and shows a solid relationship with altitude WWDSE (2008). Mean yearly precipitation fluctuates from more than 1200 mm for every year in the high-raised uplands to below 700 mm for each year in the lower regions encompassing Lake Koka. 70 to 75% of the total rainfall occurs in the main wet season.

The mean yearly temperature in the study area ranges from 16 to 22 degrees Celsius and is contrarily associated with the elevation. The relative moistness is over 50% in the wet season and beneath half in the remainder of the year. Wind speed is maximum estimated to be, above 1 m/s, in April and May and minimum in the main rainy season. The average pan evaporation is about 180 mm during the dry season of November and 75 mm in the wet season at Addis Ababa Observatory. The evaporation is observed to increase with decreasing elevation since it is related to the temperature WWDSE (2008).

3.1.3 Geology and Soil

3.1.3.1 Geology

Study area contains mostly recent alluvial sediments at the surface. The deposits are weathered basalts and tuffs from valleys upstream of the plains. The recent material is deposited by river water and the thickness varies between 5-15 m depth WRDA (1983). The alluvium covering the plains act as a seasonal aquifer. The clay content between 20 and 40% results in a permeability of around 6 m-3 m/day and retains water after floods in the wet season WRDA (1983). Groundwater levels in this shallow aquifer of the plains range between 0-5m in the wet season and 2-10 m in the dry season. The underlying and surrounding higher elevated areas consist of tertiary and quaternary volcanic units as basalts, tuffs, ignibrites and ryolites. Several faults run through the region caused by the rift system and uplift of the area allowing recharge to deep fractured volcanic aquifers WWDSE (2008). The layered volcanic outcrops of the escarpments surrounding the plains result in some local springs being present as shown on figure 2. Data on the production and location of these springs is limited.

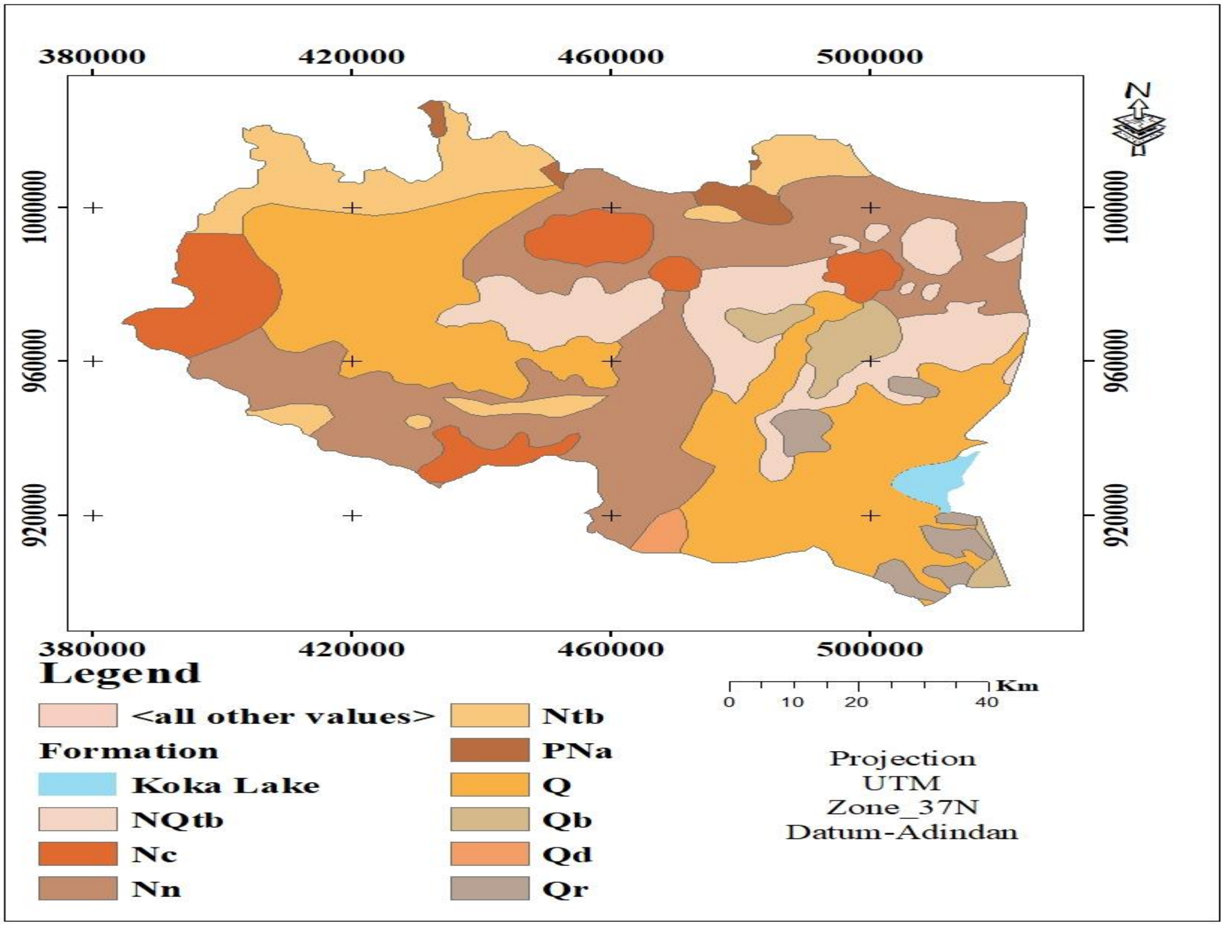

Figure 2 Geological Map of the study area: Description of the Geological units is given in the Appendix IV

3.1.3.2 Soil Map

The prevailing soil type in the study area is vertisols. The detailed study performed by Nippon (1996) gives a few assortments of the vertisols of the plains, including stagni-calcic vertisols in the longer flooded areas and the more common eutric vertisol on terraces and shorter inundated areas.

In small scale there are also fluvisols, cambisols and gleysols present on the levees and former channels of the Awash River and its tributaries. The vertisols in the Becho plain are black clays that are dominated by the montomorillonite clay mineral.

This mineral characterized by expansion during wet season and contraction when it is dry time, causing cracks at the surface in the dry season. These cracks are mainly developed in the inundated areas and back swamps of fields where they can be estimated to have a width of 10 cm and a depth of 70 cm. The hard state when dry and sticky, plastic state when wet Deckers (2001) makes tillage difficult and restricted to specific periods. Water will infiltrate quickly through the breaks with the principal downpours after the dry season, however when the muds are wet and extended the penetration is exceptionally low. The soils have a high water holding limit, permitting flood downturn farming where yields utilize the remaining soil dampness. The investigation of Nippon, (1996) did exclude the fields west of Lake Koka, however the conditions are required to be like the Becho plain. The depositional condition will for the most part be marginally higher vivacious than in the Becho plain, where enormous assemblages of stale water are available for a while. This can bring about marginally coarser dregs and comparative soils that created on the levees and previous channels of the Awash River in the Becho plain. The soil map shows that the dominant soil type in the floodplains of the Awash River is fluvisols.

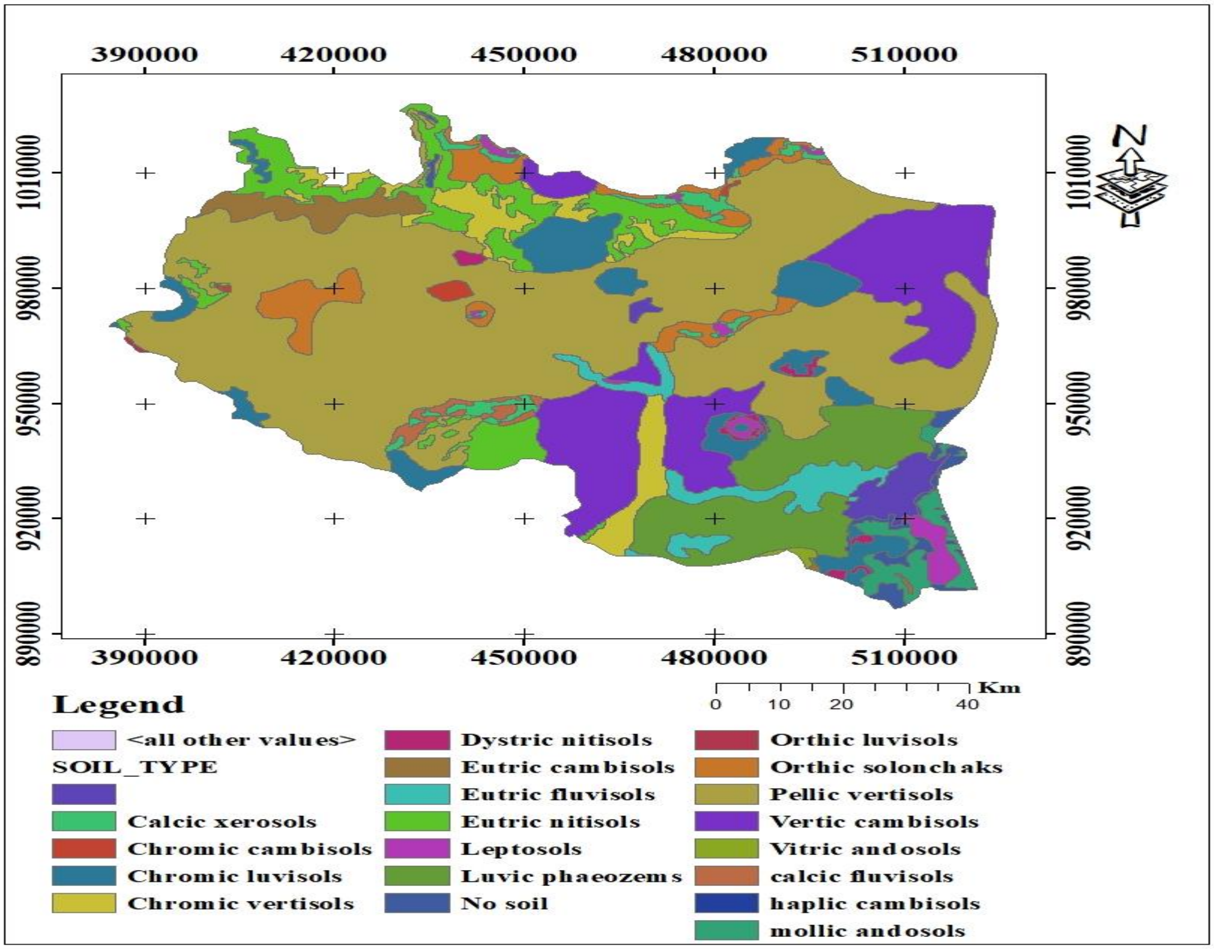

Figure 3 Soil Map of the Upper Awash Basin

3.1.4 Drainage Condition

3.1.4.1 River system

The Awash River originates from the mountain range at an altitude of 2,900m in the western most region of the basin near Ginchi town and flows south eastward. Thereafter it defiles in to the Bacho Plain which shapes an alluvial plain with a normal elevation of 2060m.After the Bacho Plain, it goes through the sloping and rugged zones to the Koka reservoir found nearly 135 km downstream of the Teji Bridge Abebe (2007).

The discharge carrying capacity and gentle gradients of the rivers in the Awash River are insufficient for discharging floods in the high wet season. The flood release overtops the waterways and streams basically into the Gebar Meda and the Dilu Meda territories, which causes an inundation of the Bacho Plain. The inundation water hence streams into the Awash River when the flood tops die down.

3.1.4.2 Characteristics of Rivers

The upper Awash river flowing down to the Koka reservoir can be classified into three stretches: the first is A 30 km stretch upstream of the Bacho Plain with a remarkably steep river bed slope ranging from, the subsequent stretch is a 60km stretch in the Bacho Plain between the Teji bridge and Kombolcha with a delicate riverbed slope and the third an approximately 90 km stretch between Kombolcha and the Koka reservoir with a steep river bed slope. Such delicate riverbed segment between the Teji Bridge and Kombolcha hinders smooth flow during the high wet season, which is one of the causes of the poor drainage conditions in the Dilu Meda and Gabar Meda areas, Abebe (2007).

3.1.5 Flooding Problem

The area with lower elevation and depressed lands Upper awash Basin are inundated every year especially during the rainy period from July to September. Some of the most inundated places in the study area includes the Bacho plain area the Dilu Meda and Gabar Meda and the downstream part of Awash river like berga (Atebela area). The inundation in these areas basically results from the overflowed water that overflows the rivers because the discharge capacity is insufficient for the high rainy season flow. Moreover, the inundated water in both these areas can't be depleted effectively because of the little conveying limit of the Awash River in the downstream of the Bacho Plain and the small drainage capacity of the bridges and culverts.

The main and serious constrains in the study area are the occurrence of recurrent inundation and floods. An impressive number of ranchers in the study area have the lands situated located in the immersion area. Their cultivating is constrained by the risks of crop losses by floods and inundation that happen a few times each blustery season because this farmers in bacho plains are involved in flood recession farming practices.

The sociological damages caused by inundation are also serious. A few settlements are regularly confined during the rainy season because of floods and due to this life is completely disrupted.

Figure 4 flood inundation around in Becho plain part of Upper Awash Basin

3.1.6 Land Use

The study area consists of 32 woredas and Addis Ababa city Administration with a population size of 5,851,656 CSA (2007). Most of the population in these woredas are involved in agriculture. The land use types in the Upper Awash Basin 75% of the land is agricultural land, 11.9% is used for grazing land and this is an area that is inundated during the rainy season, the rest of the 9.7% of the land consists of villages, roads and woodlots Nippon (1996). The main crops and agricultural practices differ in the upland areas from the inundated areas. In the Becho plain all farmers have cropland in the inundated areas with an average plot size of 2.4 ha and 88% have land in the upland areas with an average plot size of 1.75 ha Nippon (1996).

In the uplands the vast majority of the land is utilized for the teff (Eragrostis tef)(63.85 ha), chickpea (Cicer arietinum) (10.65 ha) and wheat (Triticum aestivum)(9.77 ha). These crops are planted in the beginning of the wet season and use rainwater for their growth. The low-lying immersed regions are utilized for the cultivation of lentil (Lens culinaris) (57.06 ha), chickpea (35.13 ha) and teff (31.63 ha).

3.2 data collection

3.2.1 Primary data

As a primary data ground coordinate sample points has been collected using Global Positioning System in order to identify the location of Bridges which is used as an input for HEC-RAS/HEC-GeoRAS, flood Inundation area and validate the collected ground features of earth's truth to the classified satellite image of the study area (for image classification Accuracy Assessment).

3.2.2 Secondary data

The DEM data of 12.5m resolution has been downloaded from Alaska Satellite facility and having downloaded the DEM the study area was extracted and missing data were filled in GIS environment Using a GIS extension Arc hydro tools.

The study Area is extracted from two adjacent scene satellite imageries of Path 169 Row 54 of 2017 layer stacking has been carried out in order to combine different bands. The images were the mosaicked, the Upper Awash Basin area was subsetted from the mosaicked scene and different image enhancement techniques were applied to extract the land cover information for image classification using ERDAS IMAGINE 2014 software. The study area LandUse/Landcove has been extracted from LANDSAT imagery obtained from USGS websites and Maximum likelihood supervised classification technique has been carried out using ERDAS imagine software to identify different land use land cover classes. Flood discharge data for gauging station located in different part of the study area has been collected from (MWIE).

3.2.3 Software and materials

The materials and Software that has been used in this study includes Global positioning system (GPS) for ground coordinate data collection and computer hardware and software for data analysis. The software that has been employed for preparing and analysis of the data are ERDAS IMAGINE and ArcGIS 10.5 and HEC-RAS/HEC-GEORAS for flood inundation Modelling. The thematic layer for each flood causative factor has been prepared and edited, overlaid and visualized using ArcGIS 10.5. ERDAS IMAGINE has been used for satellite image processing like geometric correction, image enhancement, image segmentation and other operations related to satellite image processing.

Table 2 Data source and Materials

NO	DATA	Source	Relevance
1	Satellite Image	LANDSAT	To extract the different Land-use data and verify the water bodies within the study
2	DEM	ALOS PALSAR DEM	For elevation and to generate slope
3	Soil map	ethio_soil map by extracting	To extract the soil types within the study Area
4	Population	Central statistics agency	For deriving population density factor
5	Flood discharge data	Ministry of water irrigation and Energy	For flood inundation mapping
6	Rainfall Data	Ethiopian Meteorological agency	For derivation of rainfall map
Software and hardware's			
7	ArcGIS version 10.5	-	for flood analysis, producing maps and statistical report generation
8	HEC-RAS/HEC-GEORAS	-	Analysis and mapping of flood inundation

3.3 Methods

The methodology of this study depends for the most part on analysis of image acquired from different sources and other data sets. The objective of this thesis is to develop a hazard and flood risk map in GIS environment and to prepare flood inundation model using HECRAS/HEC-GEORAS. To determine the flood vulnerable areas, Multi Criteria Analysis (MCA) is used.

3.3.1 Multi criteria Analysis

Multi-Criteria Analysis is a structured decision-making tool used to solve complex problems. MCA describes any deliberate and organized approach used to determine overall preferences among alternatives with the end goal of positioning them from the most important to the least important Sadequr (2014). The result of MCA is a set of weights for the different alternatives. There are various procedures of MCA and a few of them are Aggregated Indices Randomization Method (AIRM), Analytic hierarchy process (AHP), Analytic network process (ANP), Best worst method (BWM), Characteristic Objects method (COMET), Choosing By Advantages (CBA), etcetera. This thesis utilizes the Analytic hierarchy process (AHP) technique because that is the procedure which is widely used for flood analysis.

The MCA analysis was done in two phases. The first phase is the utilization of Analytic Hierarchy Process (AHP), a multi criteria decision tool, to determine the weights of the criteria. AHP constructs a hierarchy of decision criteria using comparisons between each pair of criteria formulated as a matrix. The paired comparisons produce weighting scores that indicates the hierarchy of importance of selected criteria which. The second phase then incorporates the determined weights in a weighted overlay process to produce the flood hazard map.

3.3.1.1 The Analytical Hierarchy Process

The analytical hierarchy process (AHP) is one of the multi criteria Analysis (MCA) which was employed for processing of the data. The Analytic Hierarchy Process was presented by T. L. Saaty as a multi-criteria decision-making approach in the 1970s as a method of dealing with resource and asset allocation. Saaty developed the Pair-wise Comparison Method which is utilized in the AHP to obtain the weights or priority vector of the selected criteria. To make the comparisons, a scale of numbers is needed which shows how many times one element is more important over another element with which it is being compared Saaty (1977).

Table 3 the fundamental scale of Absolute number (Saaty, 1980)

Intensity of Importance	**Definition**	**Explanation**
1	Equal importance	Two activities contribute equally to the objective
3	Moderate importance	Experience and judgment slightly favor one activity over another
5	Strong importance	Experience and judgment strongly favor one activity over another
7	Very strong or demonstrated importance	An activity is favored very strongly over another; its dominance demonstrated in practice
9	Extreme importance	The evidence favoring one activity over another is of the highest possible order of affirmation
Reciprocals of above	If activity i has one of the above non-zero numbers assigned to it when compared with activity j, then j has the reciprocal value when compared with i	A reasonable assumption
1.1–1.9	If the activities are very close	May be difficult to assign the best value but when compared with other contrasting activities the size of the small numbers would not be too noticeable, yet they can still indicate the relative importance of the activities.

To create Analytical Hierarchy Process rank needs to be assigned for each factor, this was done by consulting experts who are working in flood related professions and some other experts on agriculture and environment protection areas.

The factors that were utilized as an input to for multi-criteria analysis was preprocessed in accordance to the criteria set to develop flood hazard analysis. So Eigen vector for flood causative factors like Slope, Drainage Density, Distance to river Rainfall, Elevation, Soil and Land use/Land cover was computed using Analytical hierarchy process (AHP) of Multi-criteria Analysis.

In practice, individual decisions are never the same and do not agree perfectly therefore, the degree of consistency achieved in the scaling of the matrix is measured by a Consistency Ratio (CR) which shows the probability that the scaling were generated randomly. A CR less than or equal to 0.1 indicates an acceptable reciprocal matrix and greater than 0.1 indicates that the matrix should be reexamined Saaty (1997). Reexamining the matrix involves locating inconsistent decisions with regards to the importance of criteria and revising these decisions by comparing the pair of criteria again.

Calculating Consistency Ratio (CR)

Consistency Index (C.I) = $(\Lambda_{max} - n)/(n-1)$ where n is number of compared factors

$$C.R = (C.I)/\text{ Random index } (R.I) \quad \ldots\ldots\ldots\ldots\ldots\ldots\ldots\ldots \text{Equation 1.1}$$

3.3.2 Flood Hazard Mapping

Main causative factors for the occurrence of flooding Hazard in the study area were identified based on the existing realities and knowledge of the study area.

Flood hazard analysis of Upper Awash basin was carried out using weighted sum overlay analysis of the seven reclassified flood causative factors (i.e. reclassified rainfall, reclassified drainage density, reclassified slope, reclassified distance to river, reclassified elevation, reclassified soil and reclassified landuse Layers using Multi-criteria Evaluation technique (MCE) using model builder in ArcGIS environment.

3.3.3 Flood Risk Mapping

Flood risk is considered as a product of flood hazard (physical impact) and flood vulnerability (susceptibility to damage) Alexander (1997). Creating flood risk map includes a hazard assessment which is the attributes of event in terms of magnitude and frequency. Whereas vulnerability analysis deals with effect of event on element at risk Ilorme (2007).

Flood risk analysis was carried out by applying the following general risk equation Shook (1998).

Risk = (Elements at risk)*(Hazard*Vulnerability)……….……………………Equation 1.2

Before flood risk analysis the flood hazard analysis was performed using multi criteria evaluation (MCE). To carry out the MCE, seven flood disaster causative factors such as elevation, slope, drainage density, Distance to river, Soil, Rainfall and land-use were developed and weighted. Then weighted overlay technique was computed in ArcGIS10.5 Model Builder to generate flood hazard map.

The vulnerability is assumed to be one by considering the degree of loss to be total for the study area. Finally to generate flood risk map of the study area prepared by overlaying flood hazard map with two elements at risk layer (land use and population density) using weighted sum overlay analysis technique in ArcGIS 10.5 environment by assigning equal weight for each inputs. 100

3.3.4 Flood Inundation Modeling

3.3.4.1 Flood frequency analysis

In this thesis flood Frequency Analysis was carried out to estimate of how often a specified event will occur. FFA is most usually used by engineers and hydrologists worldwide and basically comprises of estimating flood peak quantities for a set of non-exceedance probabilities. Before the estimation is carried out determination of suitable probability distribution plays a very important role so as to get flood at different return period. Nirman (2017).

Frequency analysis is just a strategy for estimating the frequency of occurrence or probability of occurrence of past or future events. To determine the discharge of five station Akaki, Addis Alem, Awash Bello, Melka Kunture and Ombole gauging station in response to 5, 10, 25, 50, 100 and 200-year return periods flood frequency analysis was conducted based on the Daily stream flow data obtained from Ministry of water Irrigation and Energy for the year 1988 to 2012. To select the appropriate distribution a total of three distributions were compared in this study. These are Log Normal Distribution, Log Pearson Type III Distribution and Gumbel's Distribution. The comparison is based upon goodness-of-fit analysis. Based on 5, 10, 25, 50, 100 and 200- year return periods, depth of flood were used for preparation of flood inundation and flood depth maps.

3.3.4.1.1 Log Normal Distribution

The log-normal distribution has the same characteristics as the normal distribution except that the dependent variable, X, is replaced with its logarithm. The characteristics of the log-normal distribution are that it is bounded on the left by zero and it has a pronounced positive skew. These are both characteristics of many of the frequency distributions that result from an analysis of hydrologic data.

If a logarithmic transformation is performed on the normal distribution function, the resulting logarithmic distribution is also normally distributed.

If a random variable x has a log normal distribution (LN2) distribution then the log transformed variable has a normal distribution. The transformed variable is denoted by

$$Y = \ln[x] \qquad \text{Where } x>0$$

The maximum likelihood method is generally best for fitting the LN2 distribution. The maximum likelihood method ~~gi~~ves:

$$Y = 1/n \sum_{i=1}^{n} \ln(Xi)$$

$$S^2{}_y = 1/n \sum_{i=1}^{n} (\ln(Xi) - \bar{Y})^2$$

Estimate of flood flow corresponding to T-year return period can be obtained from

$$X_T = e^{(Y+ZT*Sy)}$$

Where for flood flow $Z_T = ((1-1/T)^{0.135} - (1/T)^{0.135}) / 0.1975$

Where Z_T is the standard normal variate, $\bar{y}$ is mean and S_y standard deviation of the log transformed data.

3.3.4.1.2 Gumbel's Distribution

Gumbel distribution is one of the strategies for predicting extreme hydrological events based on Maximum discharge data and is additionally one of the most commonly utilized distribution in flood frequency analysis.

As indicated by Mujere (2006), to use Gumbel's distribution the accompanying rules should be considered.

The river is less regulated i.e. not influenced by human water demand such as reservoir, diversions and urbanization.

a. Maximum flow data are homogenous and independent.
b. Observed flow data was more than 10 years with good quality.

To estimate the design flood for any return period using Gumbel's distribution the accompanying methodology were applied, as given by Chow (1988) is presented below:

Annual peak flood data for the river was assembled.

$$\text{Mean} = \frac{\sum_i^n Xi}{n} \quad \text{and} \quad Sn = \sqrt{\frac{1}{n-1}}\sum_i^n (X - X)^2 \ldots\ldots\ldots\ldots\ldots\ldots\ldots(1)$$

The values for Y_n and S_n are taken as 0.5362 and 1.1124.

Reduced variate Y_t is computed using Equation (2).

$$Y_t = -(\ln.\ln(\frac{T}{T-1})) \quad \ldots\ldots\ldots\ldots\ldots\ldots\ldots\ldots\ldots\ldots\ldots\ldots\ldots\ldots(2)$$

Flood frequency factor K is computed using the following Equation.

$$K = \frac{Yt - Yn}{Sn} \quad \text{………………………………………….. (3)}$$

The magnitude of flood for a particular return period is computed using the following equation.

$$X_T = X + K*S_n \quad \text{…………………………………………… (4)}$$

It is vital to confirm if the observed flood data collected in the basin follows Gumbel's distribution or not. So as to accomplish this, the observed data is arranged in descending order and Rank is assigned for each flood data, from the rank assigned and total number of data return period for each flood data is calculated; the reduced variate corresponding to each flood was computed using Equation (2). A plot of the reduced variate and magnitude of flood is made on ordinary graph paper. If an eye fits to this plot suggest a straight line, then it is reasonable to conclude that the Gumbel's distribution is a good fit for the observed flood data.

3.3.4.1.3 Log Pearson type III Distribution

Another distribution that has found wide application in hydrologic analysis is the log-Pearson Type III distribution. The log-Pearson Type III distribution is a three-parameter gamma distribution with a logarithmic transform of the variable.

Log Pearson Type III Distribution (LP3) distribution describes a random variable whose logarithms are P3 distributed. Thus

The method of estimating the parameters of the LP3 distribution is like that for the P3 distribution except that logarithms of the data are to be taken before estimating moments.

Thus for a set of observations (x_1 , x_2,.......x_n) the transformed data are given

$$Y_1 = \ln x_1 \; Y_2 = \ln x_2 \quad \text{…………….} \; Y_n = \ln x_n$$

Estimate of flood flow corresponding to T-year return period can be obtained from

$$X_T = e^{(Y + K_T * S_y)}$$

$$K_T = 2 / g_y (1 + (Z_T * g_y / 6) – g^2{}_x / 36)^3 - 2 / g_y$$

Where g_y is the coefficient of skewness of log transformed data.

3.3.4.2 Goodness of fit test

The goodness of fit test is a strategy which is utilized to compare the sample obtained with the type of the sample one would expect from the hypothesized distribution and to check whether the hypothesized distribution function fits the data in the sample. In this study, for evaluating the suitability of different probability distributions which were significant for predicting discharge for various return period, the following goodness-of-fit tests were adopted: (i) Kolmogorov-Smirnov test (KS); (ii) Anderson-Darling test (AD); and Q-Q Plot. The K-S and AD tests calculate test-statistics, which are utilized to investigate how well the data fits the given distribution. For K-S and AD test the goodness of fit test was performed for testing the following hypotheses:

H0: the stream flow (Discharge) data follow the specified distribution

H1: the Stream flow (Discharge) data do not follow the specified distribution.

In this thesis three types of goodness-of-fit tests have been carried out to check which distribution function fits the data in the sample. These test includes Kolmogorov-Smirnov test, Anderson-Darling test at significance level (α=0.05) along with Q-Q plot for choosing the best fit Probability distribution Sharma et al. (2010).

3.3.4.2.1 Kolmogorov-Smirnov Test

The KS test is used to decide if a sample comes from a hypothesized continuous distribution and is based on the empirical cumulative distribution function. Kolmogorov-Smirnov test statistic (D) is a function of the greatest vertical distance between distribution functions, either hypothesized or empirical distribution functions. A hypothesis is rejected if the test statistic is greater than the critical value at a chosen significance level. For the significance level of α=0.05, the critical value calculated was generated by Easy fit software. The samples are assumed to be from a CDF F(x). The test statistic (D) is:

$$\boldsymbol{D} = \mathbf{max}(\boldsymbol{F}(\boldsymbol{xi}) - \frac{\boldsymbol{i-1}}{\boldsymbol{n}}, \frac{\boldsymbol{i}}{\boldsymbol{n}} - \boldsymbol{F}(\boldsymbol{xi}))$$

3.3.4.2.2 Anderson-Darling test

The Anderson-Darling test compares an observed CDF to an expected CDF. This method gives more weight to the tail of the distribution than KS test, which in turn leads to the AD test being stronger, and having more weight than the KS test. The test rejects the hypothesis regarding the distribution level if the statistic obtained is greater than a critical value at a given significance level (α). The significance level most commonly used is α=0.05, producing a critical value of 2.5018. This number is then compared with the test distributions statistic to determine if it can be rejected or not. The AD test statistic (A2) is:

$$A^2 = -n-1/n \sum_{i=1}^{n}(2i-1)[\ln F(x_{(i)}) + \ln(1- F(x_{n-i+1}))]$$

3.3.4.2.3 Graphical display

Graphical display is also an effective way to determine whether the fitted distributions are consistent with the given set of observations Stedinger (1993). Probability plots (or quantile-quantile plots) are a methods for comparing observed data to a theoretical distribution.

To develop the quantile-quantile plot (Q-Q plot), each xi:n was paired with yi:n, which is computed from the assumed cumulative distribution function (CDF), F(x). The set of points (xi:n, yi:n) is plotted on normal graph with a 1:1 straight line extending from the origin. Theoretically, all points expected to fall on the 1:1 line if the assumed CDF is the true distribution Tao (2002).

3.3.4.3 Generation of RAS Geometry Layer

The river geometry layers like stream center lines, River bank line, flow path center lines, bridge, and cross section cut lines were digitized from the 12.5 resolution DEM of ALOS PALSAR. This is a pre-processing HEC-GeoRAS stage which includes creating these attributes in GIS, and then geometric layers were exported to the HEC-RAS the geometry file. In HEC-GeoRAS, each attribute (geometric features) is stored in a separate feature class called as RAS Layer.

River/reach name, station to each cross section was assigned based on the intersection with the stream centerline. Bank station locations to each cross section were assigned. Lastly, reach length was assigned based on the flow path lines using downstream reach length menu.

The elevation for each cross-section was extracted from the terrain model. The elevation extraction Process converts the 2-D features to 3-D features. This process results in the generation of a new feature class.

3.3.4.4 Importing and Editing Geometric files

At this stage the Geometric files that were generated from Geo-RAS in GIS were imported to HEC-RAS, the Geometric data prepared from GeoRAS may have some error so this errors needs to be edited this process was performed in HEC-RAS.

Surface roughness value (manning's value) which affects the characteristics of river were assigned in a HEC-RAS tool. The values were filled in HEC-RAS manning's value to the left bank, right bank and stream center lines. Each characteristic was given n-value based on table values for 48 Similar conditions Cowan (1956) and engineering judgment using field survey photos of the study area. Maximum flow data computed for different return periods using Log Pearson distribution was entered in the steady flow module for the profiles of 50, 100 and 200 in HEC-RAS. Finally, Plan data was carried out which contains information to the run specifications of the model, including a description of the flow regime.

3.3.4.5 Flood plain delineation

Flows were defined at the most upstream location each tributaries and junction of Awash River. Each flow that needs to be simulated (profiles) were defined for different return periods of 50, 100 and 200, then estimated discharge for the respective return period has been fed into the profile in HEC-RAS. To define downstream boundary, normal depth slope was defined using reach boundary condition tool in HEC-RAS.

Water surface profile were computed for the flow data defined in different profiles. Then after successful steady flow simulation HEC-RAS results were exported to ArgGIS for inundation mapping in the form of SDF file format. Finally water inundation for the respective water surface profile were created using profile with 50,100 and 200 years return period flow.

CHAPTER FOUR

DATA ANALYSIS

4.1 Flood Hazard Assessment

At data analysis stage, all the factor layers are ready to be combined in order to assess the flood hazard zones in the study area. If all datasets were equally important, it could be possible to combine them simply. However, from the principal eigenvector calculation, the relative importance of each parameter was determined. Therefore, the higher the weight, the more influence a particular factor will have in the flood generation. Accordingly, the factor layers were combined by applying the following formula in the raster calculator of spatial analyst extension in ArcGIS environment. It was done systematically using ArcGIS model builder.

To produce the flood hazard map weighted sum overlay has been carried out in a GIS environment. This process requires a spatial data for the criteria being used for the weighted overlay process. The criteria that are considered as flood causative factors in this thesis are; Elevation, Rainfall intensity (precipitation), Drainage Density, Elevation, Slope, distance to River, soil type and Land use/cover. Raster maps for elevation, slope, and drainage are derived from ALOS PALSAR DEM which has a resolution of 12.5m. A raster map is created for precipitation through surface interpolation Inverse distance weight (IDW). Soil Map has been collected from Ethiopia Ministry of water irrigation and energy.

The following flood causative factors were combined for the development of flood hazard map by using Model builder in ArcGIS environment.

4.1.1 Slope

The slope raster was derived from the DEM using the ArcGIS Spatial Analyst extension of surface module, which enabled to classify the area according to the steepness and the gentleness of the terrain. The Slope function could calculate the maximum rate of change between each cell and its neighbors. Every cell in the output raster had a slope value. The lower the slope value, the flatter the terrain was and the higher the slope value the steeper will be the terrain.

The low-lying area with low slope angle will be inundated first as compared to the high slope area during flooding. Those area with steep slope show high peak discharge as compared to the low-lying area and causes the depletion of the storage in the upstream areas.

Then the slope raster was reclassified in to five sub group using the natural breaks (jenks). The reclassified slope was given a value 1 to 5 with the higher value of 5 showing high influence, resulting in very high flood rate, while the lower value of 1 showing very low influence, resulting in very low flood rate. The break values and the description of the new slope classes are given in Table 4 below.

The ALOS PALSAR DEM data was subjected to substantial pre-processing operations. The basic problem is the voids or missing data which affect the quality of the data. Voids are resulted from shadows and layover. This mostly occurs in the mountainous region where there are poor signal returns and smooth areas like water and sand which reflect little energy to the radar. It was processed to fill in the voids in Arc-GIS and the final processed map is used for slope conversion in degree.

Table 4 Slope Classification for the study area

Slope(Degree)	**Rank**	**Level of Hazard**
0-3	5	Very High
3-8	4	High
8-14	3	Moderate
14-23	2	Low
23-74	1	Very low

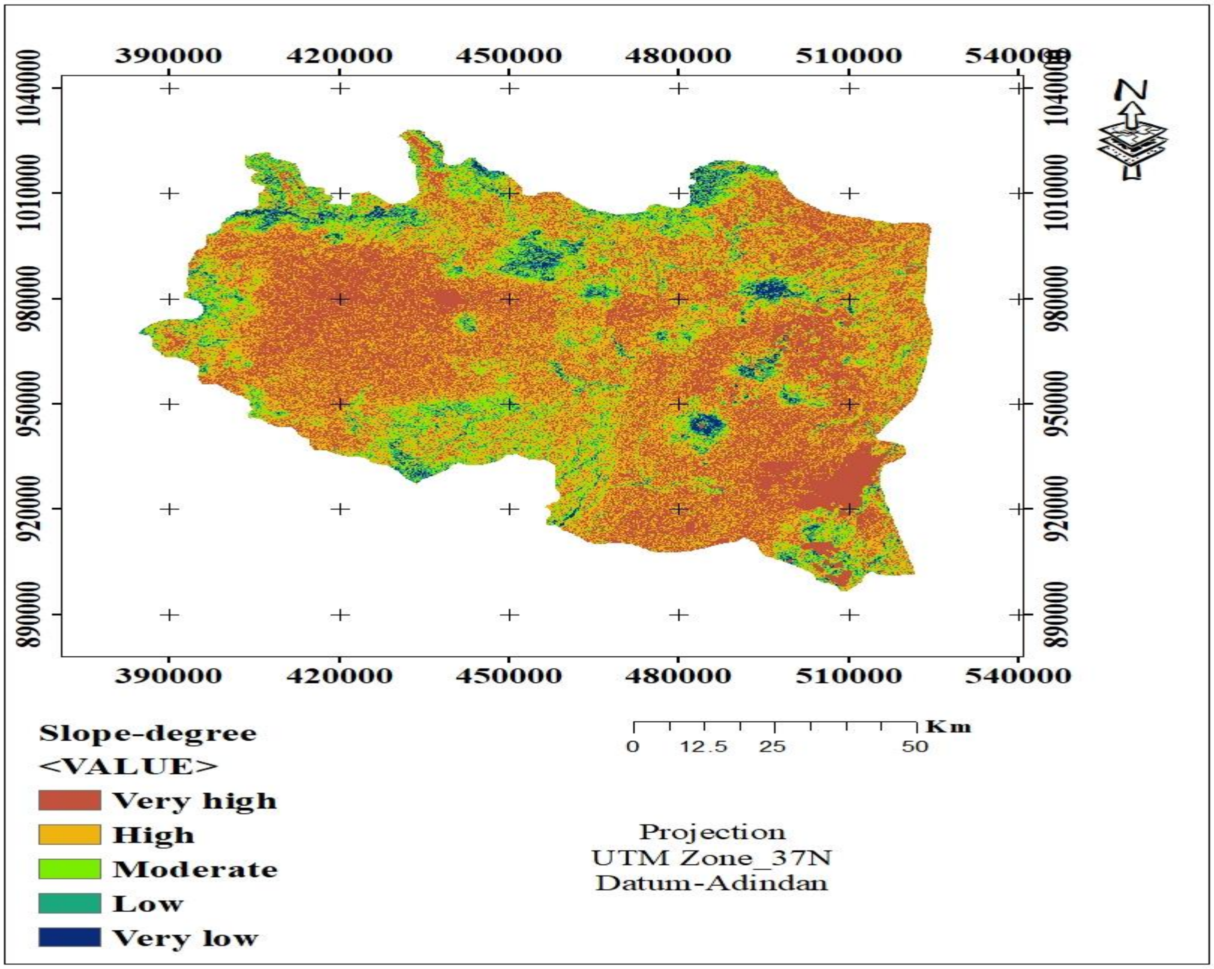

Figure 5 Reclassified Slope Map of upper Awash basin

4.1.2 Drainage Density

Drainage system, which develops in an area, is strictly dependent on the slope, the nature and attitude of bedrock and on the regional and local fracture pattern Alemayehu (2007).Drainage density (DD) a fundamental concept in hydrologic analysis is defined as the ratio of the length of drainage per basin area. Drainage density is controlled by permeability, erodability of surface materials, vegetation, slope and time.

Drainage density is an inverse function of infiltration Ajin (2013). Greater drainage density indicates high runoff for basin area along with erodible geologic materials, and less prone to flood. Thus the rating for drainage density decreases with increasing drainage density.

Table 5 Drainage density Reclassification value

Drainage Density(KM/KM^2)	Rank	Level of Hazard
0-0.07	1	Very high
0.07-0.17	2	High
0.17-0.26	3	Moderate
0.26-0.36	4	Low
0.36-0.83	5	Very low

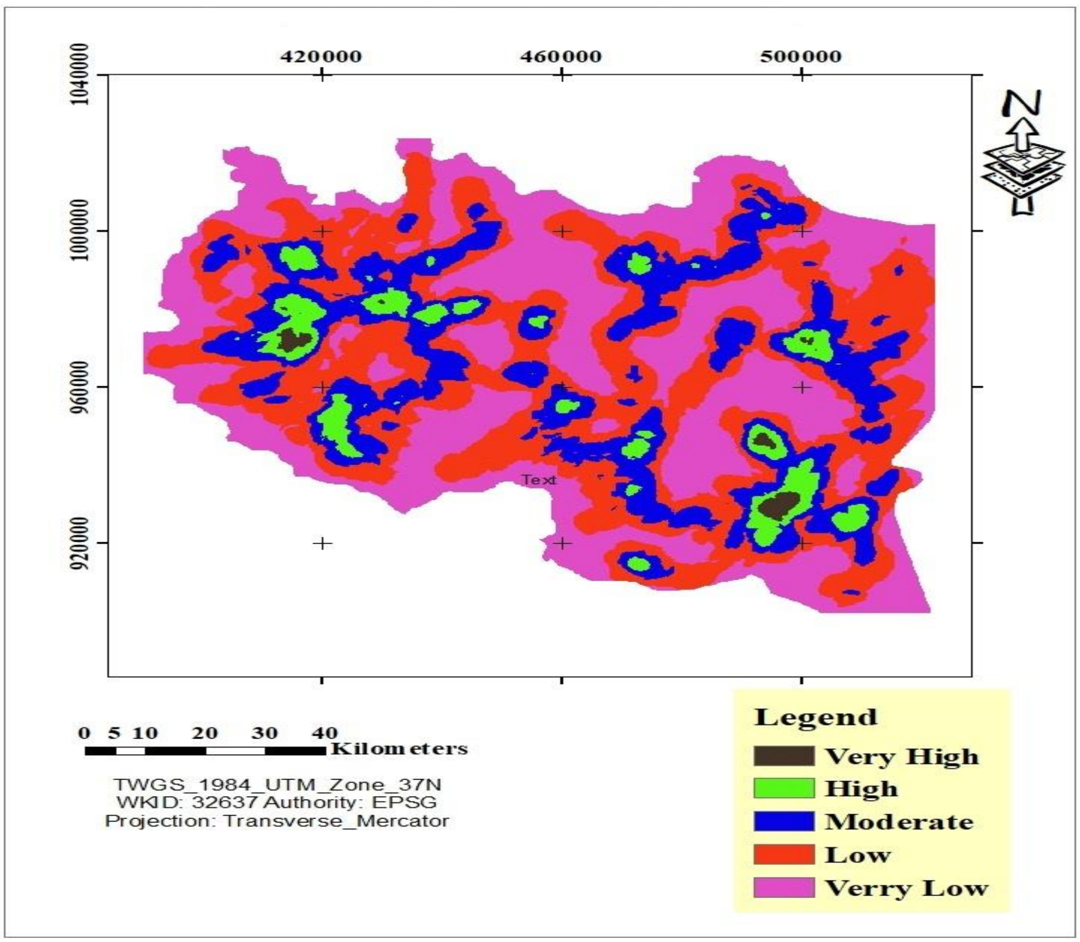

Figure 6 Reclassified drainage density map of upper Awash basin

DEM was used to extract the drainage network, to calculate the drainage density of the streams. Arc Hydro10.5 software, which works as an extension on ARC GIS 10.5 version software was used to generate drainage network map of the sub-basin. Using the spatial analyst, line density module was used to compute drainage density of the sub-basin. Line density module calculates a magnitude per unit area from poly line features that fall within a radius around each cell. The density layer is further reclassified in five sub-groups using standard classification schemes namely quantiles. This classification scheme divides the range of attribute values into equal-sized sub ranges, allowing you to specify the number of intervals while Arc Map determining where the breaks should be. Finally, the drainage density was reclassified into continuous scale in order of flood hazard rating. The drainage density in the sub-basin ranges from 0.071 to 0.825 km/km2.

4.1.3 Rainfall Data

The annual average of the rainfall data from 1988-2018 has been downloaded from the center of Hydrometeorology and Remote Sensing (CHRS) Portal developed by University of California. It uses neural network function classification/approximation procedure to compute an estimate of rainfall rate at each 0.25^0 $*25^0$ pixel of the infrared brightness temperature image provided by the geostationary satellites. The PERSIANN (Precipitation Estimation from Remotely Sensed Information using Artificial Neural Networks) system was based on geostationary infrared and later extended to include the use of both infrared and daytime visible imagery. The downloaded grid format rainfall data was converted to point data average of twenty five year data was calculated. Spatial interpolation of rainfall from the point data has been carried out using an Inverse Distance Weighted (IDW) technique. IDW interpolation determines cell values using a linearly weighted combination of a set of sample points. Then the interpolated surface was converted to raster layer, which was finally reclassified into five classes using equal interval scheme as shown in table below. The reclassified rainfall was given a value 1 to 5 with the higher value 5, showing high influence resulting in very high flood rate, while the lower value 1, showing very low influence resulting in very low flood rate.

Therefore, an area with very high rainfall was ranked as 5 and an area with very low rainfall was

Ranked as 1. Accordingly, the raster and the reclassified rainfall data are shown below in figure below.

Table 6 Reclassified Rainfall data value

Rainfall in mm	Rank	Level of Hazard
877.02-972.48	1	Very Low
972.48-1067.94	2	Low
1067.94-1163.39	3	Moderate
1163.39-1258.86	4	High
1258.86-1354.32	5	Very High

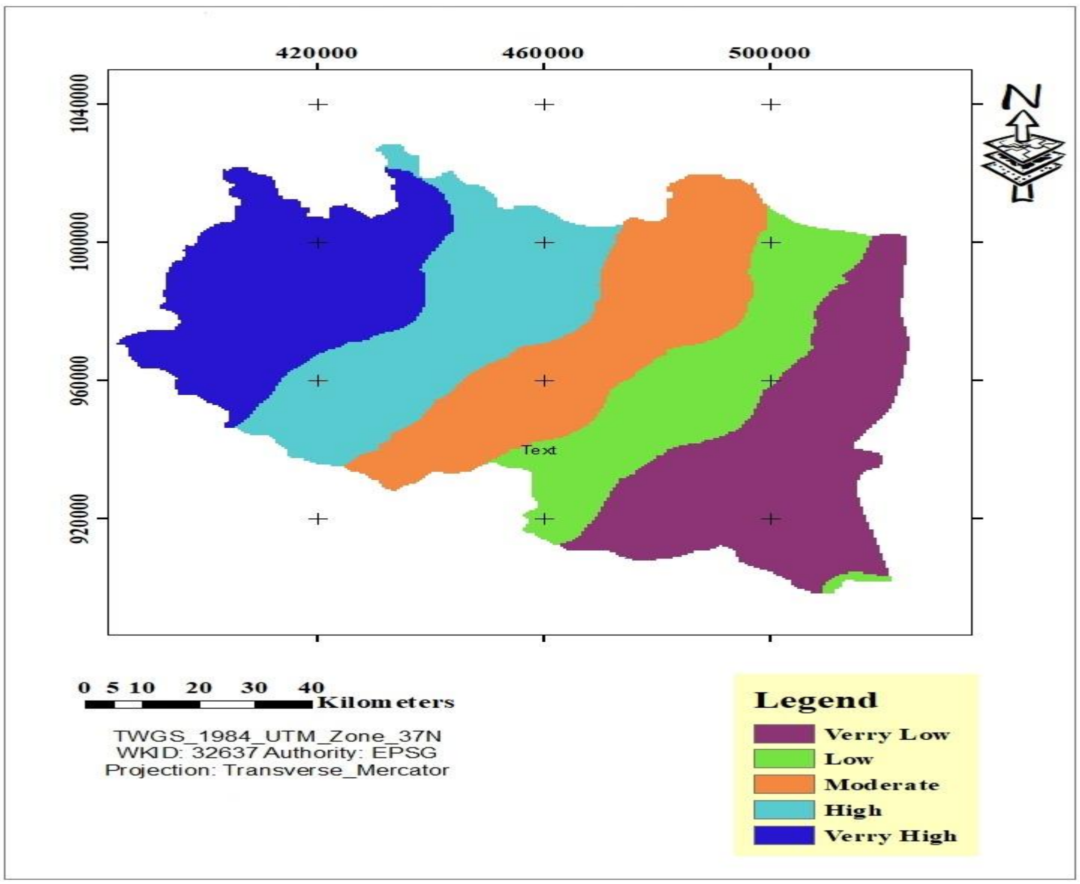

Figure 7 Reclassified Rainfall Map of upper Awash Basin

4.1.4 Elevation Factor

The raster Elevation was derived from filled DEM which has a resolution of 12.5 in a GIS environment using 3D analyst tool. The resulting raster had elevation values. Then the elevation was reclassified into five groups using equal interval scheme. Based on their susceptibility to flooding, the lower the elevation value the higher the flood hazard was and the higher the elevation value the lower was the flood hazard. The rank and the level of hazard of the elevation classes are given in Table 7 below.

Table 7 Reclassified Elevation value of the study area

Elevation	Rank	Level of Hazard
1538-1944	5	Very High
1944-2350	4	High
2350-2756	3	Moderate
2756-3162	2	Low
3162-3568	1	Very Low

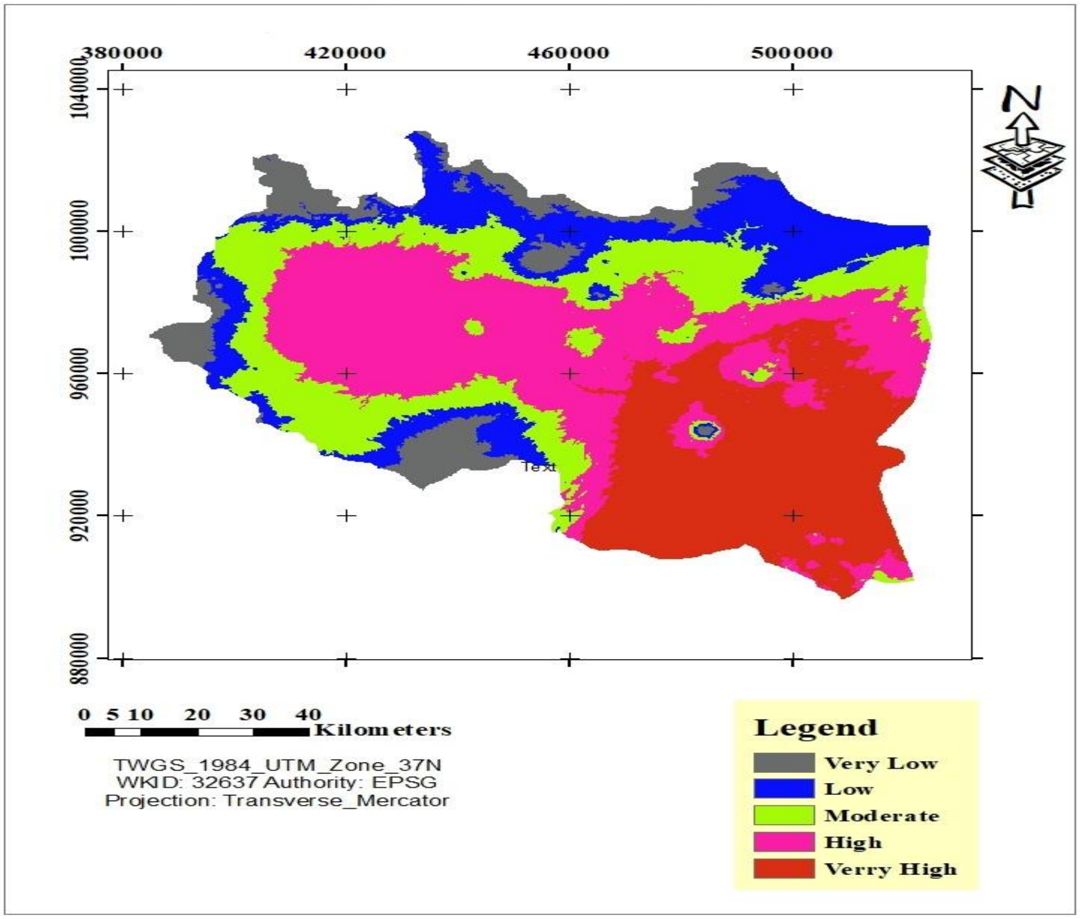

Figure 8 Reclassified Elevation Map of upper Awash basin

4.1.5 Distance to River

The distance to active channel is one of the contributing factor in flood hazard assessment. These channels have been buffered by considering the distance up to which damage to life and property can be significant. This will also help to locate the distances from active channel for the safe evacuation of the people at risk. The distance to the active channel has been computed by buffering on at 500 m both sides of the channels with spatial analyst and 3–D analyst. After buffering, the values were divided into four classes with respect to hazard assessment namely, very high (0-1000m), high (1000-1500m), moderate (1500-2000m), low (2000-300) and very low (>3000m) based on our field experience.

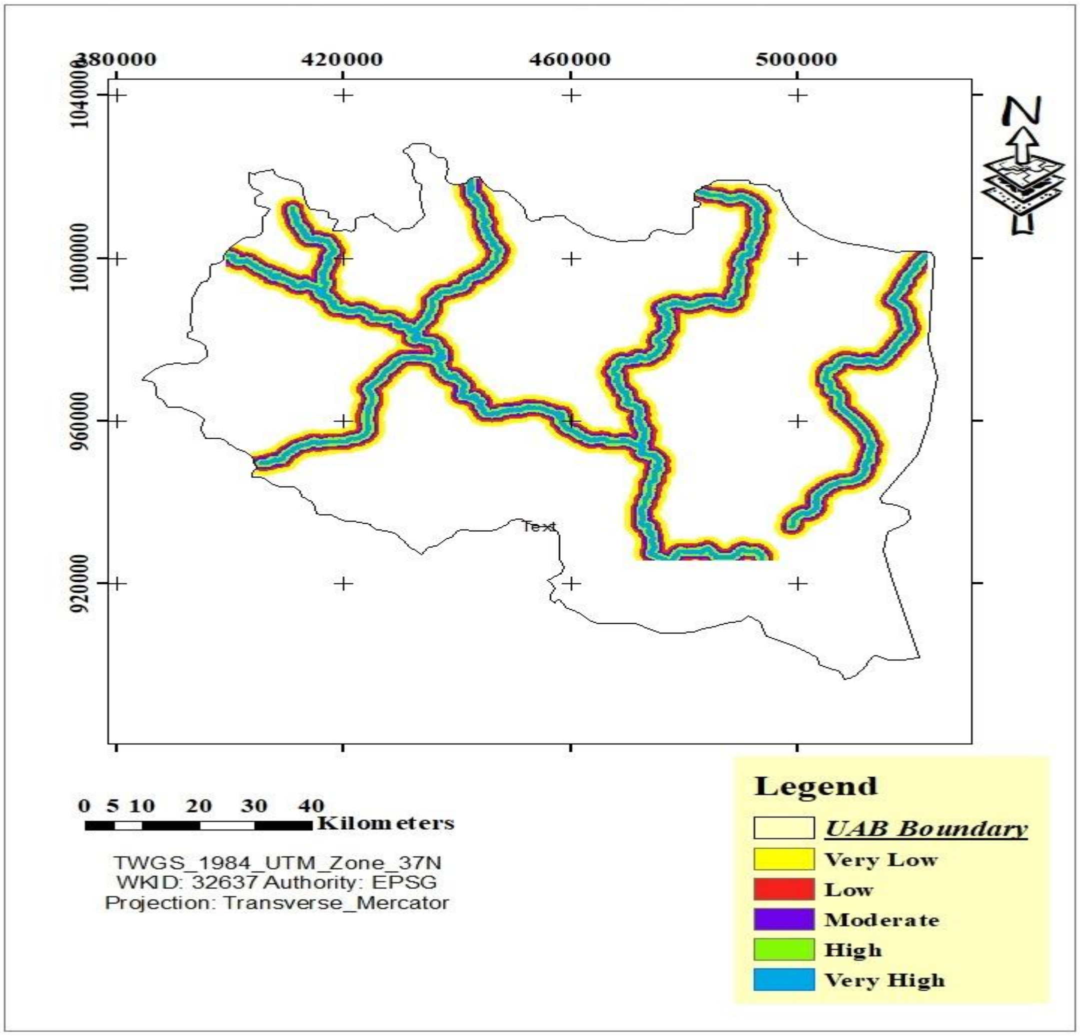

Figure 9 Reclassified Distance to River Map

4.1.6 Land Use/ Land Cover Factor

The land use of the study area was classified from the subsetted image using two adjacent scene of Landsat 8 acquired on 01/10/2017 and 01/17/2017, having path and row of 169/54. Before classifying the satellite image different image processing like layer stacking, image enhancement and histogram equalization has been carried out in ERDAS imagine 2014 software and ArcGIS environment. Then the Land use/Land cover class has been identified from the subsetted image using one of the classification techniques supervised classification with the aid of 250 sample points using signature editor.

Supervised Classification using maximum likelihood classifier (MLC) was carried out for Landsat-8 image for the year 2017. MLC classifies the image based on the information contained in the in the signature. The layer assigned with name "Landuse Landcover". The available LULC include six different categories namely: agriculture, forests, Buit-up area, Barren-Land, and water bodies as shown in figure below. The landcover classes represent feature on the land surface while landuse represents the activities within which the landcover is being used. This is the classification scheme of selecting the representative areas with the help of the spectral characteristic of the feature in the image. The accurate and complete classes to be defined in the supervised classification is critical in case of coarse resolution image.

Classified pixels were clustered into the following five general categories: Built-up Area, Agricultural lands, forest, barren-land and water bodies. As shown in figure below. Then each of the land use types was further reclassified for the overlay analysis. Accordingly, Built-up area, was given more weight, which is equal to 5, water bodies was given weight 4, Barren land was given weight of 3, agricultural land was given weight 2 and Forest was given weight of 1.

The error matrix of the image classification was computed to determine the accuracy of classified image. The assessment was carried out using 250 reference points collected using hand GPS from the field and by using an input of satellite image for checking. From the result overall accuracy of 86.4 % was achieved with a kappa coefficient result of 0.83. The detail for accuracy assessment is given in the Appendix III A.

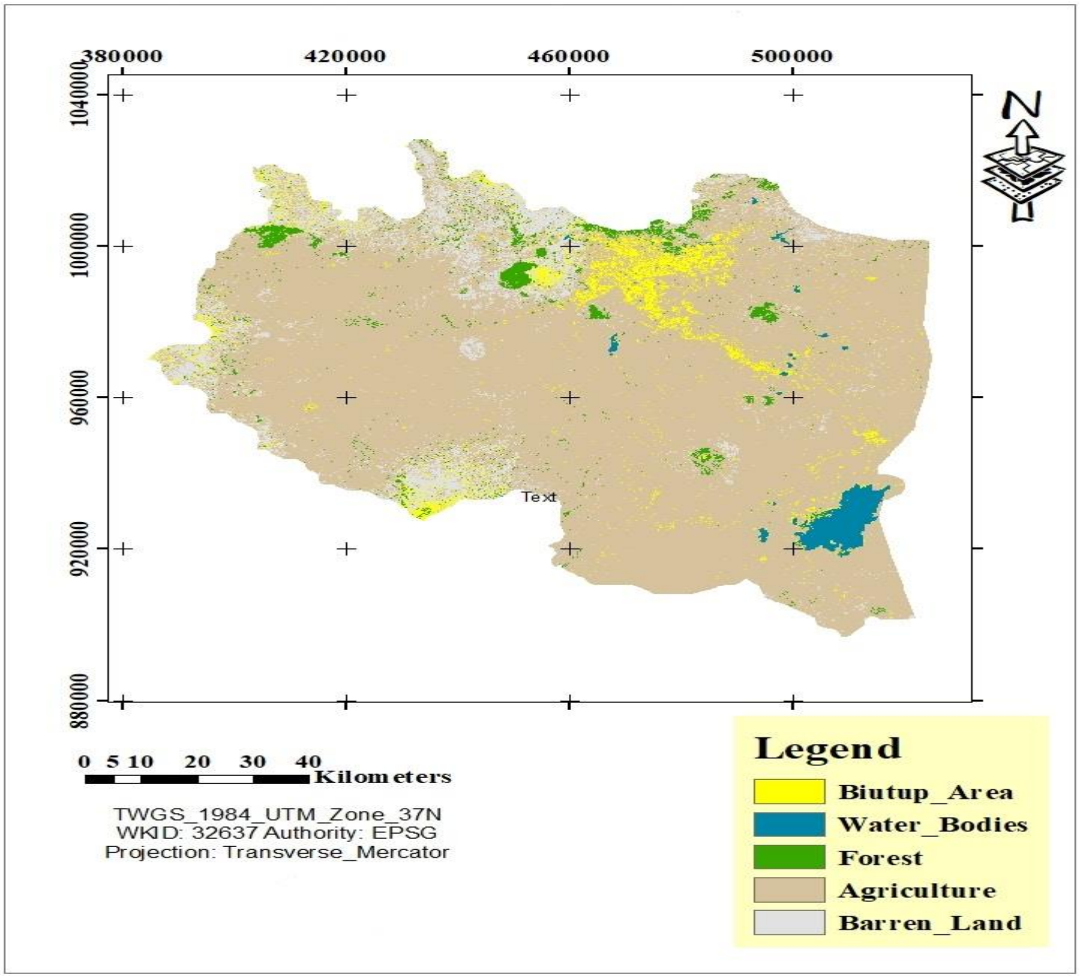

Figure 10 Land use land cover map of upper Awash basin

The LULC statistics below show that the major part of the study area is dominated by agriculture land 8430.14 sq.km which is 75% of the study area. This is followed by Barren areas 1383.97 sq.km, which is 12.33 % of the total area. Built-up area covers the third level with an area of 938.36 sq. km which is 8.4% of the total area.

The study area is almost flat with gentle slope mostly suitable for agriculture. The area of forest cover is very less which is estimated to be around 302.88sq km which is about 2.7% of total area.

Table 8 Area of Different Land use Land cover class

LULC type	**AREA Sq. Km**	**Area %**
Forest	302.89	2.7
Agriculture	8430.14	75.08
Water-body	172.70	1.54
barren-land	1383.97	12.33
Built up-area	938.36	8.35
Total	**11,228.06**	**100**

4.1.7 Soil

Different soil types have different capacities to infiltrate water. Morgan (1995) stresses that "infiltration is a key component that significantly influences the rainfall -runoff process and plays an important role in controlling the amount of water that will be available for surface runoff after a rain storm event".

The soil factor of the study area was derived from the FAO standard classification of Ethiopian soil. The characteristics of each soil group are analyzed based on hydrologic soil grouping system. Accordingly, the soil group of the study area was grouped into five general classes and converted to raster format. Further, the soil raster layer group was reclassified into five groups. And new values reassigned in order of their flood hazard rating. Soil type that has very high capacity to generate very high flood rate is ranked to 5 and the one with very low capacity in generating flood rate is ranked to 1; therefore, Pellic Vertisols are ranked to 5, Chromic Vertisols are ranked to 4, Chromic Luvisols are ranked to 3, Euthric Nitosols are ranked to 2, and Lithosols are ranked to 1.

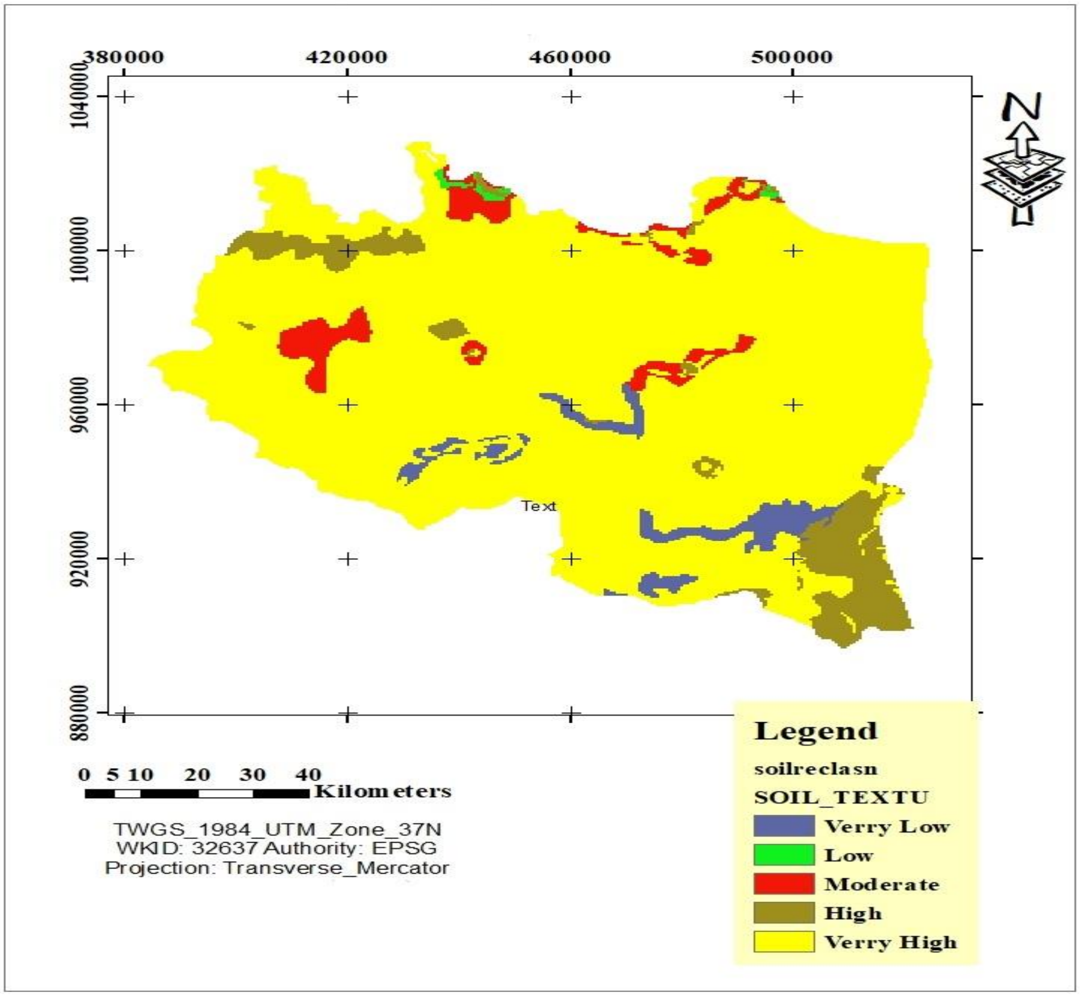

Figure 11 Reclassified Soil Map of the Study area

4.2.2 Pairwise Comparison Method

The criteria for analysis are the element which deemed to have causative influence over flooding in the basin. Matrix is constructed for these flood causative factors based on Eigen vector principles. The computed weight value of each flood causative factors is given below. Detail for computation is given in Appendix IV.

Table 9 Weight computed by Eigen vector principles

Factors	Slope	D/ce-River	Drng dnsty	Rainfall	Elevation	Soil	LULC
Weight	0.27	0.21	0.17	0.13	0.11	0.06	0.05

$$\Lambda_{max} = 7.49$$

Consistency Index (C.I) = (Λ_{max} –n)/(n-1)   where n is number of compared factors

= (7.49 –7)/(7-1)

= 0.0817

Consistency ratio (C.R) = Consistency Index (C.I)/ Random index(R.I)

Where R.I is obtained from Table

The factors being compared in this analysis are seven and the corresponding R.I value is 1.32

Table 10 Random Index value

N	1.2	3	4	5	6	7	8	9	10	11	12	13	14	15
RI	0.00	0.58	0.90	1.12	1.24	1.32	1.41	1.45	1.49	1.51	1.48	1.56	1.57	1.59

Source (Satty)

Consistency ratio (C.R) = 0.0817/1.32

= 0.061

Since the consistency ratio is less than the standard (0.061 < 0.10) our matrix is reasonably consistent so the calculated criteria weight will be used for further processing in weighted overlay.

4.3 Weighted Overlay Analysis

The weighted overlay process consist of three conceptual steps. First, each raster layer is assigned a percentage weight (the criteria weights determined in the AHP), to underscore the relative importance of each layer in the analysis. Second, the values within each raster layer are ranked (suitability scale) to allow comparison of the different types of information in each raster layer and then third, all raster layers in the analysis are overlaid. The ranking value of individual raster cells is multiplied by its layer weight and totaled with the values of other raster cells it overlays. In ranking step, every criterion under consideration was ranked in the order of preference. There are two typical ways of ranking; straight ranking (that is; most important = 1, least important = 9) or the inverse ranking (most important = 9, least important = 1). The ranking applied to this analysis corresponds to the level of flooding, which are, very high = 5; high = 4, moderate = 3; low = 2 and very low = 1.

The weighted overly tool in spatial analyst is applied for the analysis. The seven reclassified raster layers are weighted based on the weights of the pairwise comparison process and then combined based on the assigned rankings used in the reclassification. The cell values of each input raster are multiplied by the raster's weight then the resulting cell values are added to produce the final output raster. The output raster is a flood hazard map that shows which areas falls within the different levels of flooding defined above.

At this stage, all the factor layers are ready to be combined in order to assess the flood hazard zones in the study area. If all datasets were equally important, it could be possible to combine them simply. However, from the principal eigenvector calculation, the relative importance of each parameter was determined. Therefore, the higher the weight, the more influence a particular factor will have in the flood generation. Accordingly, the factor layers were combined systematically using ArcGIS model builder.

4.4 Flood Risk Assessment

Flood risk analysis is computed by Weighted Overlay setting equal importance to all factors as shown in the following table. The developed factors for overlay are Flood hazard analysis layer and the two elements at risk in the study area these are Population density and land use for flood risk analysis.

Table 11 factors for flood risk assessment

Factors	Weight	Sub-factors	Ranking
Flood hazard	0.33	very low low moderate high very high	1 2 3 4 5
Population density	0.33	108 – 243.69 243.69 – 1454.38 1454.38– 3722.62 3722.62 – 5261.32 5261.32 – 9903.03	1 2 3 4 5
Land use types	0.33	Forest Agriculture Water Bodies Barren Land Built-up Area	1 2 3 4 5

4.4.1 Population Density

The population at risk is one of main factor that needs to be considered to evaluate the loss caused due to the flooding in an affected area. To quantify the assets under potential threat, the woreda wise population density has been chosen as an important variable. Woreda shape of upper Awash basin is updated with population data from census of (2007) which is downloaded from the website of Ethiopian Central statistics Agency. Gross population density calculation method is used to calculate the number of person per square kilometers for each woredas. Right after updating, population shape file was converted to raster layer in GIS environment using using Conversion Tools/ Feature to Raster. Then further the data layer was reclassified into fiver sub-factors which are classified using equal interval method. And new values re-assigned in order of increasing number of population that is more susceptible to flood hazard.

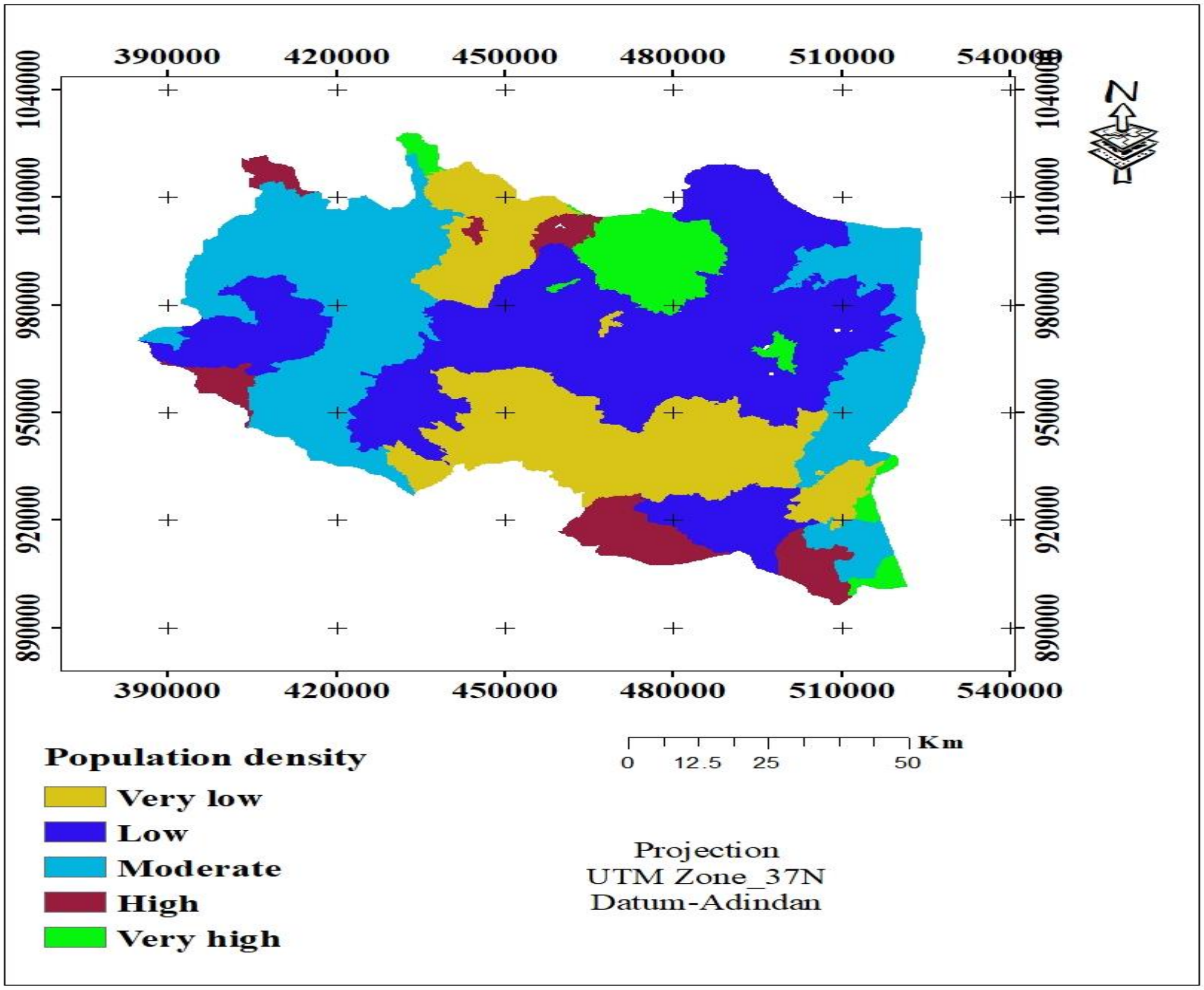

Figure 12 Reclassified population density map of the study area

4.5 Flood Inundation Modeling

For inundation mapping frequency analysis was carried out to estimate discharge for different return periods. Discharge for return period of 5, 10, 25, 50, 100, and 200 has been calculated using three probability distribution these are Lognormal, Log Pearson type 3 and Gumbel Distribution. From these distribution Log-Pearson type III distribution was selected as best distribution for estimating discharge for the above return periods using probability plotting position and statistical goodness of fit test.

4.5.1 Flood frequency Analysis

Frequency analysis is merely a procedure for estimating the frequency of occurrence or probability of occurrence of past or future events Yitea (2015). To determine the discharge of five gauging station Addis Alem, Awash Bello, Akaki, Melka Kunture and Ombole gauging station in response to 5, 10, 25, 50, 100 and 200-year return periods flood frequency analysis was carried out based on the Daily stream flow data obtained from Ministry of water Irrigation and Energy for the year 1988 to 2012. There are different types of methods for the estimation of Flood Frequency Analysis (FFA). In this study Gumbel's Distribution, Log Normal Distribution and Log Pearson type III Distribution has been used for predicting extreme hydrological events for different return periods. The result for the respective procedure for these methods are given below.

4.5.2 Goodness of fit test

Different tests of goodness-of-fit have been employed for selection of best tit distribution to estimate discharge for different return periods. In this study three distributions have been tested in order to find the best fitting distribution. The result of the test indicates that the Log-Pearson type 3 distribution function has been identified as the best fitting distribution for flood data in the awash river, based on probability plot and goodness of fit (GOF) test.

The selection of the best fit probability distribution for daily maximum discharge of each station, was performed based on the methodology described by Olofintoye et *al*. (2009). According to this methodology first, each distribution was ranked based on minimum test statistic value. The distribution holding the first rank was selected for each test independently. Then each distribution was given score based on their rank, the test ranked first was assigned the maximum score and next rank was assigned the next lower score and so on in descending order. The evaluation of all the probability distributions was carried out based on the total test score obtained by combining score of all tests. Summing the individual score of each distribution for every test category, the total test scores were obtained and hence, we identified the best fit distribution on the basis of highest score obtained. In this thesis the distribution holding the first rank was assigned a random score 15, and the next rank was assigned a score of 14 and so on in descending order.

For the selection of best fit distribution(s), we applied Kolmogorov–Smirnov, Anderson–Darling, and Quatile-Quantile plot (Q-Q plot) tests in EasyFit software. The results obtained from the test are given in Tables 12, 13, 14, 15, and 16. Anderson–Darling goodness-of-fits for given data of all river station in (Table 12-16) ranked LP3 at 1 followed by Gumbel Max Distribution at 2 and LogNormal Distribution ranked as 3 for. However test result of Kolmogorov–Smirnov ranked LogNormal Distribution at 1 (Table 3) followed by LP3 and Gumbel Max at 2and at 3 respectively. and the rest are the same as Anderson-Darling test by ranking LP3 at 1, Gumbel Max at 2 and LogNormal distribution at 3 as shown from Table 12-Table 16.

Table 12 Addis Alem Gauging station Goodness of fit test

Distribution	Kolmogorov Smirnov critical value at $\alpha_{0.05}$ = 0.26404			Anderson-Darling critical value at $\alpha_{0.05}$ =2.5018		
	Statistic	Reject	Rank	Statistic	Reject	Rank
Gumbel	0.13198	No	3	0.2998	No	3
LogNormal	0.11667	No	2	0.23551	No	2
Log-Pearson 3	30.10091	No	1	0.18389	No	1

Table 13 Awash Belo Gauging station Goodness of fit test

Distribution	Kolmogorov Smirnov critical value at $\alpha_{0.05}$ = 0.26404			Anderson-Darling critical value at $\alpha_{0.05}$ =2.5018		
	Statistic	Reject	Rank	Statistic	Reject	Rank
Gumbel	0.18197	No	3	1.299	No	3
LogNormal	0.17628	No	2	0.96517	No	2
Log-Pearson 3	0.17332	No	1	0.9029	No	1

Table 14 Akaki Gauging station Goodness of fit test

Distribution	Kolmogorov Smirnov critical value at $\alpha_{0.05}$ = 0.26404			Anderson-Darling critical value at $\alpha_{0.05}$ =2.5018		
	Statistic	Reject	Rank	Statistic	Reject	Rank
Gumbel	0.09671	No	3	0.30574	No	3
LogNormal	0.07883	No	1	0.18687	No	2
Log-Pearson 3	0.08044	No	2	0.1735	No	1

Table 15 Hombole Gauging station Goodness of fit test

Distribution	Kolmogorov Smirnov critical value at $\alpha_{0.05}$ = 0.26404			Anderson-Darling critical value at $\alpha_{0.05}$ =2.5018		
	Statistic	Reject	Rank	Statistic	Reject	Rank
Gumbel	0.06735	No	3	0.1095	No	3
LogNormal	0.07117	No	2	0.10203	No	2
Log-Pearson 3	0.06722	No	1	0.0935	No	1

Table 16 Melka Kunture Gauging station Goodness of fit test

Distribution	Kolmogorov Smirnov critical value at $\alpha_{0.05}$ = 0.26404			Anderson-Darling critical value at $\alpha_{0.05}$ =2.5018		
	Statistic	Reject	Rank	Statistic	Reject	Rank
Gumbel	0.15054	No	3	0.2998	No	3
LogNormal	0.14176	No	2	0.57219	No	2
Log-Pearson 3	0.13676	No	1	0.52864	No	1

Table 17 Melka Kunture Gauging station Goodness of fit test

Distribution	Kolmogorov Smirnov critical value at $\alpha_{0.05}$ = 0.26404			Anderson-Darling critical value at $\alpha_{0.05}$ =2.5018		
	Statistic	Reject	Rank	Statistic	Reject	Rank
Gumbel	0.1834	No	3	2.2116	No	3
LogNormal	0.15264	No	2	1.0378	No	1
Log-Pearson 3	0.08796	No	1	0.19338	No	2

The Q-Q plots was used to visually inspect the degree of fit for the distributions. From the visual point of view, there was very little difference to choose among the various distributions for representing the data used in the study. From The Q-Q plot was plotted for the data of all gauging stations pointed out that Log-Pearson type has fitted better than the LogNormal and Gumbel distributions as most of the observations fall on and around the straight line and few points are little bit far away from the fitted line. In many cases, it was hard to find out the best one from visual display of Q-Q plot. Hence, the decision was also made based on the K-S and Anderson-Darling statistical test to find out the best fit distribution more accurately.

The test Based on the above assumption indicates that the Q-Q plot for Log-Pearson distribution is best fits as compared to Lognormal and Gumbel distributions for all gauging station data sets as shown in APPENDIX V.

4.5.3 Predicted Discharge using best fit Distribution (Log-Pearson 3 Distribution)

Discharge for the return period of 5,10,25,50,100,200 years was computed using the best fit distribution obtained from the goodness of fit test which is LogPearson Type III (LP 3) distribution. The estimated discharge for Addis Alem, Awash Belo, Melka Kunture, Hombole and Akaki Gauging stations has been computed using LP3 for the respective return period as shown in the following tables.

Table 17 Predicted Discharge for Awash Belo Gauging Station

Return Period	**Probability (%)**	**Frequency Factor**	**Y=Ym+KS**	**Xi=Q(m3/)**
5	20	0.83	1.69	49.44
10	10	1.30	1.73	53.36
25	4	1.83	1.76	58.05
50	2	2.23	1.79	61.76
100	1	2.51	1.81	64.64
200	0.5	2.81	1.83	67.82

Table 18 Predicted flood Discharge for Melka Kunture Gauging station

Return Period	Probability (%)	Frequency Factor	Y=Ym+KS	Xi=Q(m3/)
5	20	0.84	2.59	394.02
10	10	1.28	2.67	467.71
25	4	1.74	2.75	561.12
50	2	2.04	2.80	630.98
100	1	2.31	2.85	700.91
200	0.5	2.56	2.89	771.91

Table 19 Predicted flood discharge for Addis Alem Gauging Station

Return Period	Probability (%)	Frequency Factor	Y=Ym+KS	Xi=Q(m3/)
5	20	0.83	1.84	69.20
10	10	1.30	1.93	85.55
25	4	1.83	2.03	108.14
50	2	2.22	2.11	128.45
100	1	2.51	2.16	145.81
200	0.5	2.81	2.22	166.65

Table 20 Predicted flood for different return period for Ombole Gauging station

Return Period	Probability (%)	Frequency Factor	Y=Ym+KS	Xi=Q(m3/)
5	20	0.84	2.74	553.24
10	10	1.28	2.80	636.77
25	4	1.76	2.87	740.15
50	2	2.07	2.91	815.92
100	1	2.34	2.95	890.80
200	0.5	2. 60	2.98	965.72

Table 21 Predicted Discharge for Akaki Gauging Station

Return Period	Probability (%)	Frequency Factor	Y=Ym+KS	Xi=Q(m3/)
5	20	0.83	2.56	376.48
10	10	1.30	2.63	413.82
25	4	1.83	2.66	459.40
50	2	2.22	2.69	496.05
100	1	2.51	2.72	524.90
200	0.5	2.81	2.75	557.10

4.5.3 Flood Plain delineation

The DEM (digital elevation model) was processed to create the TIN (triangular irregular network). After that, river geometry information like the river cross-sections, stream centerline, stream bank lines, flow paths and Bridges/culverts were extracted from the TIN for the HEC-GeoRAS model. At the same time, the land use was processed to get the Manning's n value for the individual cross-sections. After the RAS geometry data preparation, the HEC-GeoRAS model was used to generate the RAS GIS import file (final river geometry file) that can be used as input for HEC-RAS.

Before inundation map were prepared checking of cross-section; editing the river geometry, and making final correction of the river geometry file in the HEC-RAS model has been performed. After the compilation of the final river geometry file, the calculated discharge data for different return period were imported from five gauging stations into HEC-RAS and the HEC-RAS generated water surface level for different return periods has been prepared. The water surface level for each return period has been imported into HEC-GeoRAS for the generation of final inundation area map along the river.

4.5.5 Flood Vulnerability Analysis

The vulnerability maps for Upper Awash Basin flood areas were prepared by intersecting the land use map of the area with the flood inundation map which was modeled for different return periods. The result of the model depicts the vulnerability aspect of the flood risk in the particular area in terms of the presence or the absence of flooding of a particular return period.

Most of the areas upper Awash River basins are Agricultural land with less proportion of built-up area, forest, bare land and water bodies. From these land use classes most of the land about 90% of the flood inundated areas are covered by agricultural land as shown in the following figures from figure 23-figure 25. The remaining part about 10% of the area inundated by flood are built-up area and bare land are. From the analysis it is also observed that Becho plain is one of the most inundated place in the study area due to its flat topographic nature as shown on Appendix V.

Table 22 Area (Ha) of flood hazard level of 50 year return period for different Land Use Class.

Hazard Level	**Buitup-Area**	**Forest**	**Water-Bodies**	**Agriculture**	**Bare-Land**
Very low	53.66	0.63	77.10	1943.38	42.98
Low	19.55	0.36	1.18	404.77	4.80
Moderate	10.41	0.18	0.54	177.63	1.63
High	8.42	0.00	0.09	68.95	0.00
Very High	2.90	0.00	0.00	18.82	0.00

Table 23 Area (Ha) of flood hazard level of 100 year return period for different Land Use Class.

Hazard Level	**Buitup-Area**	**Forest**	**Water-Bodies**	**Agriculture**	**Bare-Land**
very low	34.48	0.27	70.94	1383.51	34.57
Low	36.65	0.54	7.96	953.05	13.48
moderate	14.66	0.36	0.90	261.70	2.99
High	8.96	0.00	0.09	74.38	0.00
very high	2.35	0.00	0.00	16.65	0.00

Table 24 Area (Ha) of flood hazard level of 200 year return period for different Land Use Class.

Hazard Level	**Buitup-Area**	**Forest**	**Water-B**	**Agriculture**	**Bare-Land**
very low	39.91	0.36	75.20	1593.18	38.55
Low	29.23	0.54	4.98	746.55	10.50
moderate	20.09	0.36	1.36	362.78	3.53
High	8.42	0.00	0.00	53.84	0.00
very high	1.81	0.00	0.00	12.85	0.00

CHAPTER FIVE

RESULTS AND DISCUSIONS

5.1 Flood Hazard

In this study, the flood hazard zone of the study area was delineated by considering the seven parameters. The final combined resulting map obtained after the weighted overlay analysis was flood hazard map of the study area Fig below. From this map, the different levels of flood hazard in the study area was calculated and given in Table below. The result has revealed that, 9.18 % of the basin was characterized by very high flood hazard level and 36.09 % of the study area was characterized by high flood hazard level. On the other hand 45.14 % of the study area fall under moderate hazard level zone. The rest of the study area which is 9.46 % and 0.14 % falls under low and very low hazard level respectively. On the basis of historical information, the upper part of Upper Awash basin becho Woreda was the most commonly inundated area due to its geomorphic settings as it comprises of topographically flat land.

Areas of different Woredas in the Basin that are subjected to different flood hazard levels were also calculated. The further analysis for flood hazard for different woredas of the upper awash basin is shown in Appendix III.

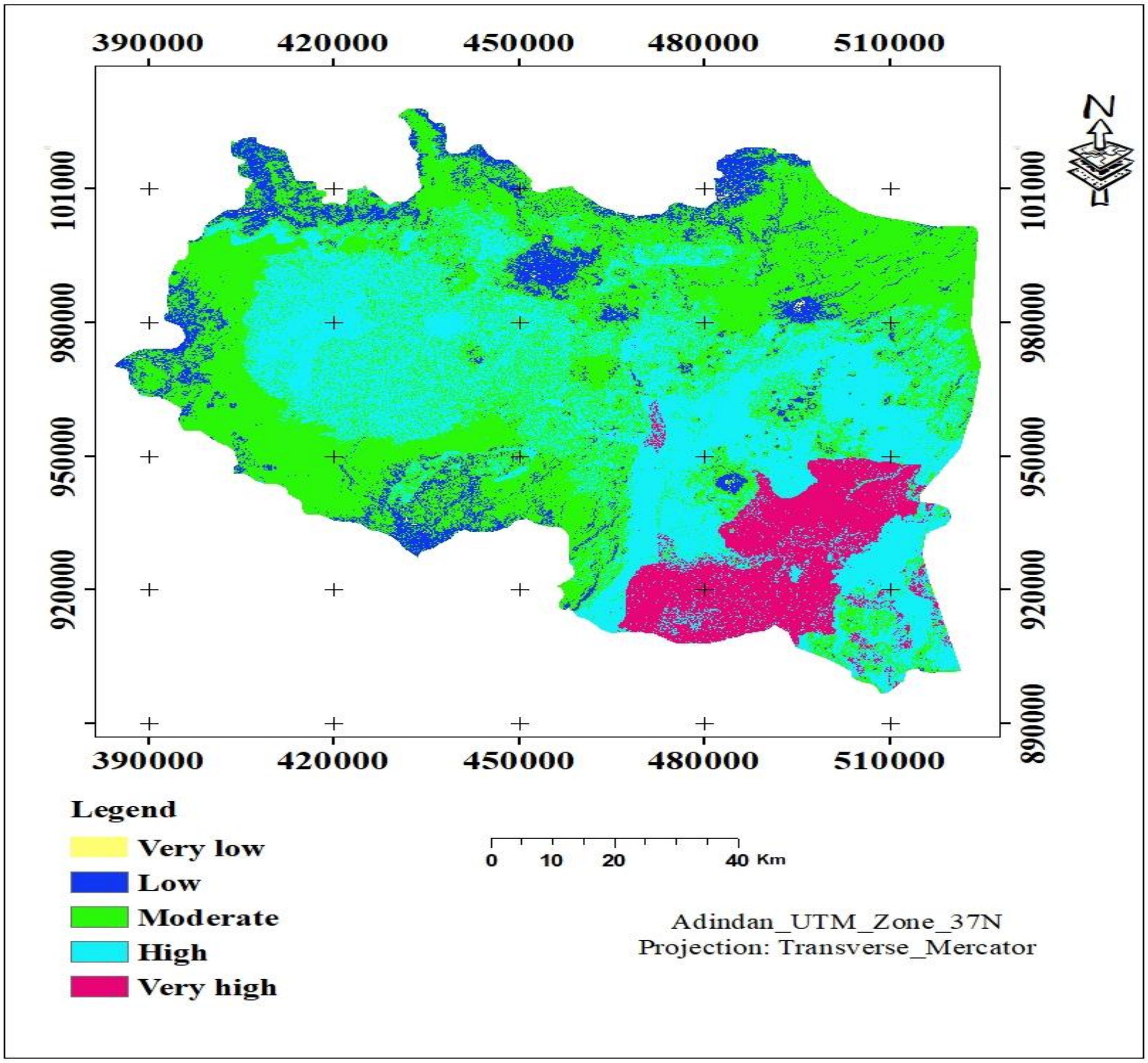

Figure 13 Flood Hazard Map of Upper Awash basin

Table 25 Table flood hazard level of Upper Awash basin

Hazard Level	**AREA (Sq.Km)**	**Area (%)**
Very low	15.70	0.14
Low	1061.91	9.46
Moderate	5068.10	45.14
High	4051.89	36.09
Very high	1031.14	9.18
Total	**11228.74**	**100**

Flood hazard level for different land use land cover class revealed that agricultural land is more subject to flood hazard. The further analysis for flood hazard in each land use land cover class is given in the following tables 26.

Table 26 cross tabulated area (sq.km) of land use class by flood hazard level

Hazard Level	**Land use land cover types**				
	water bodies	**Forest**	**Bare-land**	**Farm-land**	**Built-up**
Very low	0.01	8.56	1.06	6.06	0.00
Low	0.74	77.97	57.06	887.27	3.70
Moderate	10.76	29.02	327.89	4599.01	99.13
High	159.16	0.44	174.44	3619.69	97.22
Very high	2.27	0.00	63.57	952.20	13.06
Total	172.95	115.98	624.01	10064.22	213.11

5.1.1 Validation of Flood hazard map

Validation of flood hazard map has been carried out by using point data collected during field visit in the study area. The data was collected through observation of flood recession land and by interviewing people in the area. The result indicates that 38.49 and 51.32 percent of the point collected from field fall under high and very high flood hazard level. The point were collected randomly and detail result of cross tabulation of point data with flood hazard layer is sown in the following table 27.

Table 27 Cross tabulation of points with flood hazard map

Hazard level	**number of points**	**percent**
very low	0	0
Low	5	1.89
Moderate	86	32.45
High	166	62.64
very high	136	3.02
Total	265	100

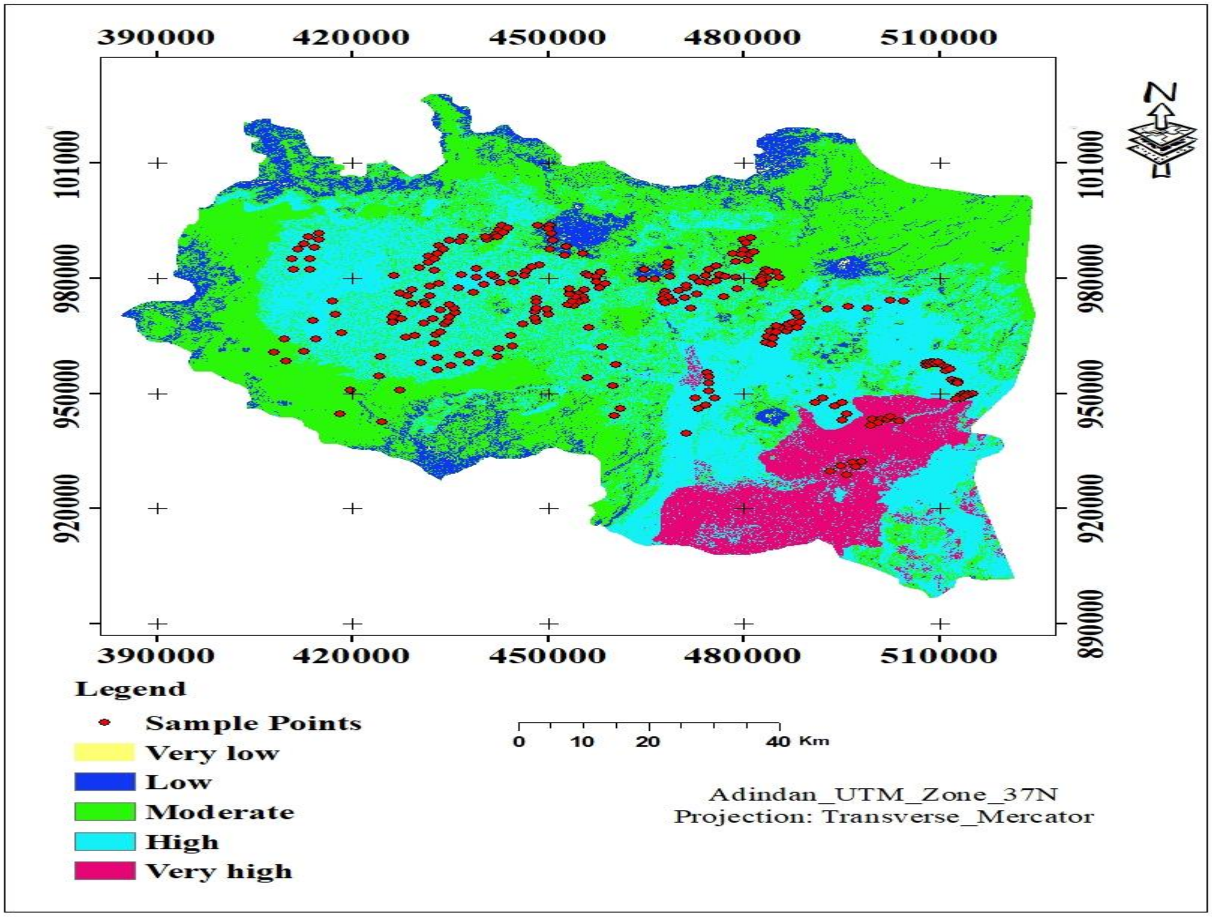

Figure 14 Validation map for flood hazard

5.2 Flood Risk

Flood risk analysis is computed by Weighted Overlay setting equal importance to all factors (Fig). The developed factors for overlay are Flood hazard analysis layer and the two elements at risk of the study area which are Population density and land use for flood risk analysis.

According to the flood risk map (Figure 27), it was estimated that 4.43, 15.73, 41.35, 28.82 and 9.67 percent of the area considered in the upper awash basin were subjected respectively to very low, low, moderate, high and very high flood risk. Further analysis for element at risk and risk in each woreda is given in Appendix III.

Table 28 Flood Risk level for different land use types

Risk Level	Area(sq.km) of Land use type				
	Water bodies	Forest	Bare-land	Agriculture	Built-up
Very low	166.37	100.19	70.27	149.66	1.39
Low	0.52	8.05	244.79	1466.32	15.96
Moderate	3.23	5.46	182.61	4452.61	68.65
High	0.39	1.82	75.65	3048.45	77.78
Very high	0.57	0.12	41.08	995.04	49.00
Total	171.07	115.64	614.42	10112.07	212.77

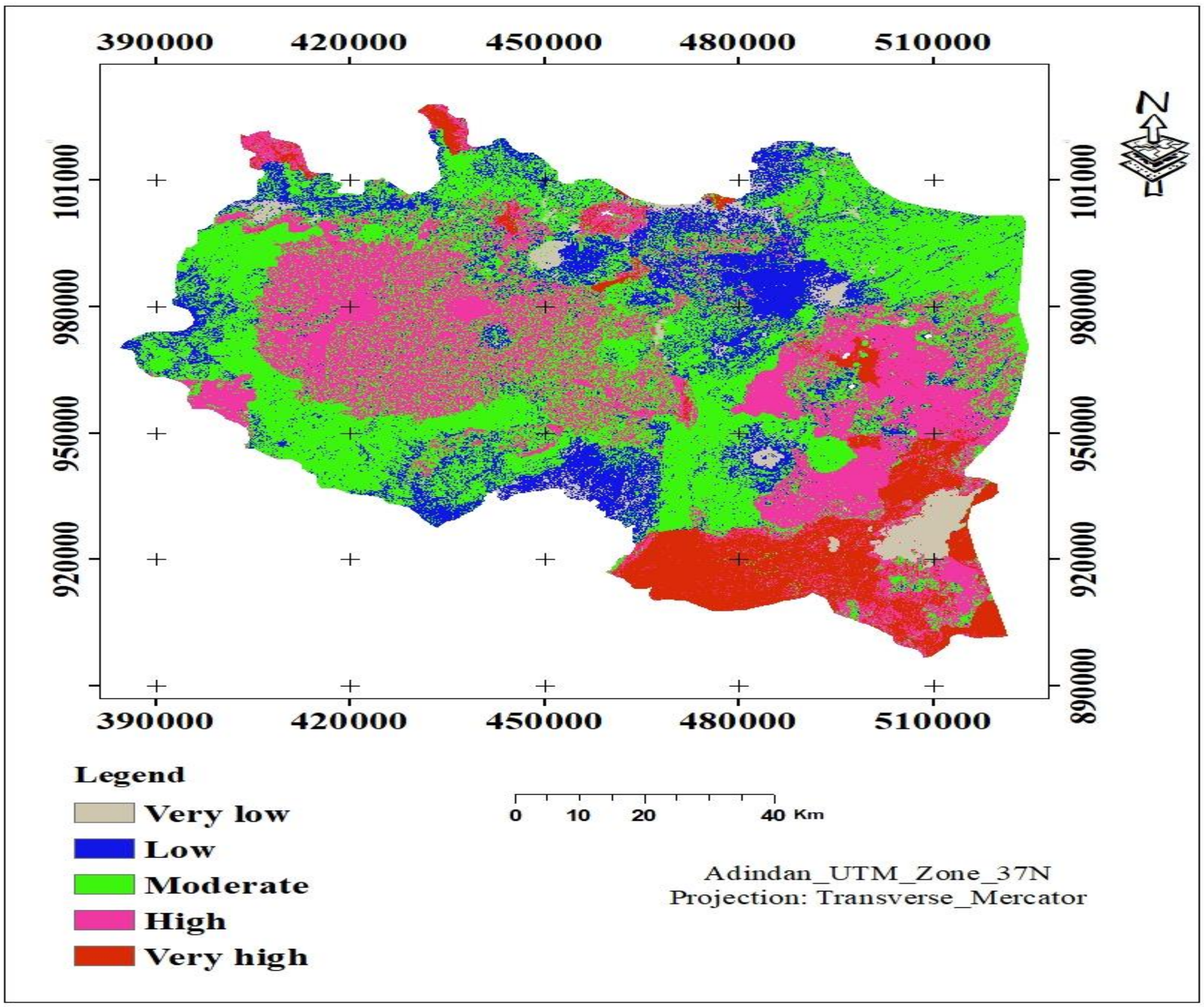

Figure 15 Flood Risk Map of Upper Awash Basin

Further analysis for flood risk assessment revealed that 0.10% of forest, 9.84% of Agriculture, 6.69% of Barren Land and 23.03% of Built-up area of the upper awash basin fall under very high flood risk level, and it is also observed that 1.57% forest, 30.15% Agriculture, 12.31% barren land and 36.56% Built-up land use land cover of the study area are classified in to high flood risk levels. The result of detail analysis is given in table 28.

5.3 Flood Extent Map

From inundation analysis it is observed that most flood depths for the return period of 50, 100, and 200 are in range of 0.00-0.70m, 0.00-1.50 and 1.70 with a flood depth covers 74.63%, 52.37% and 58.34% of the total flood extent. The next highest portion is covered by a depth of 0.70-1.20m, 1.50-2.50m and 1.70-3m which is about 15.07%, 34.50% and 26.17% of the total area respectively. On the other hand the highest flood depths is >3m, >4.5 and >6m which covers 0.71%, 0.45% and 0.46% which covers smallest portion of total flood extent map respectively. Inundation extent map for different return period is shown on figure 19, figure 20 and figure 21 below.

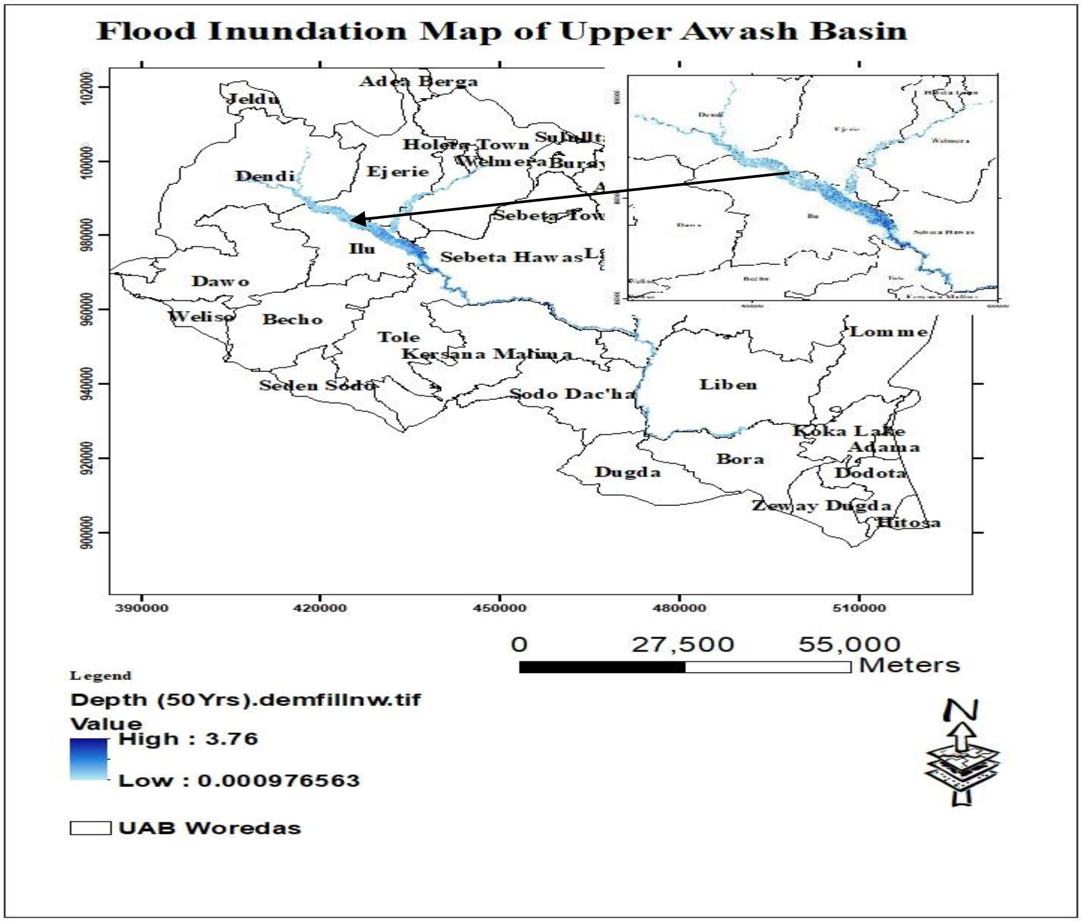

Figure 16 flood depth map for 50 year return period

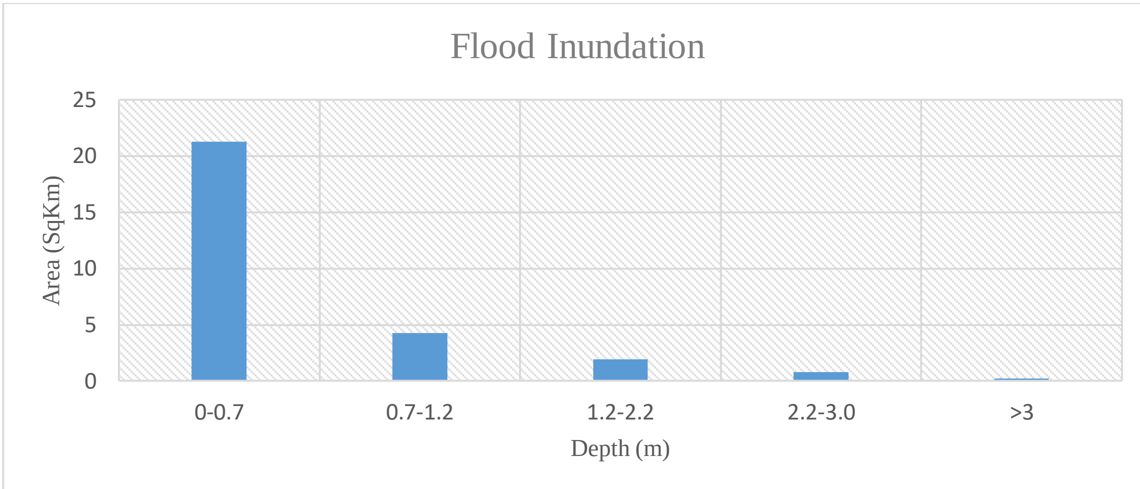

Figure 17 Depth of flooded Area for 50 year return period

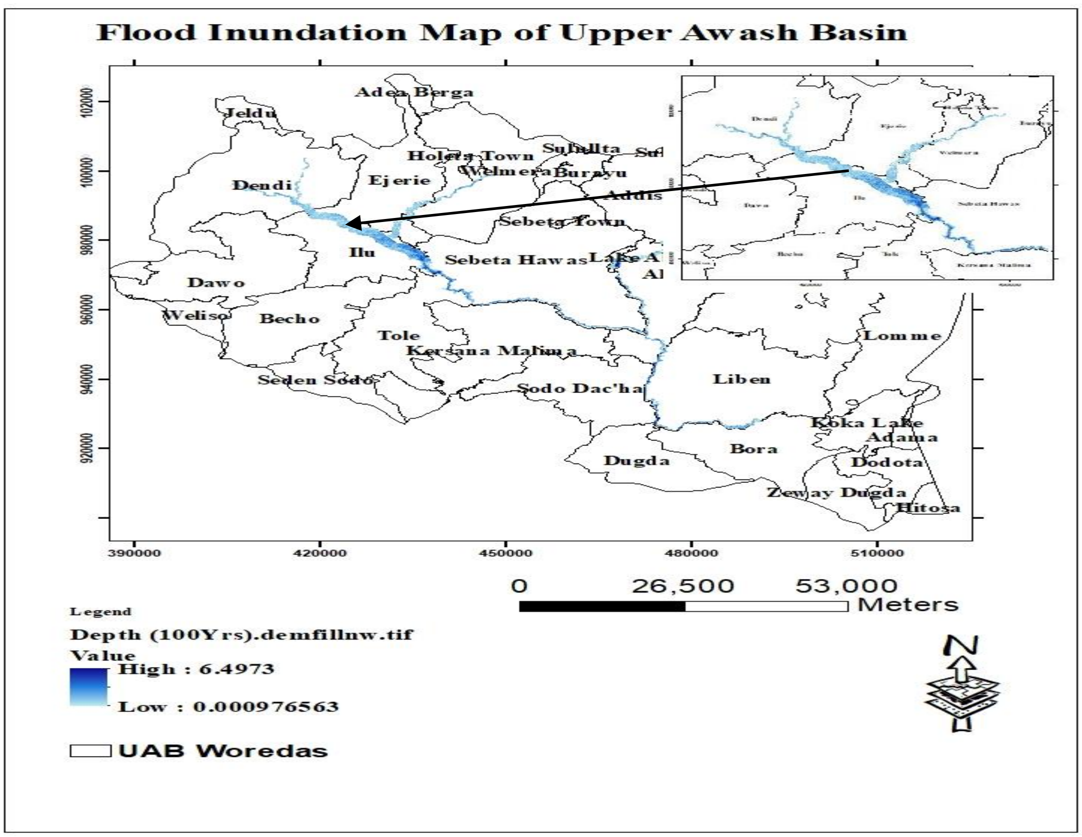

Figure 18 flood depth map for 100 year return periods

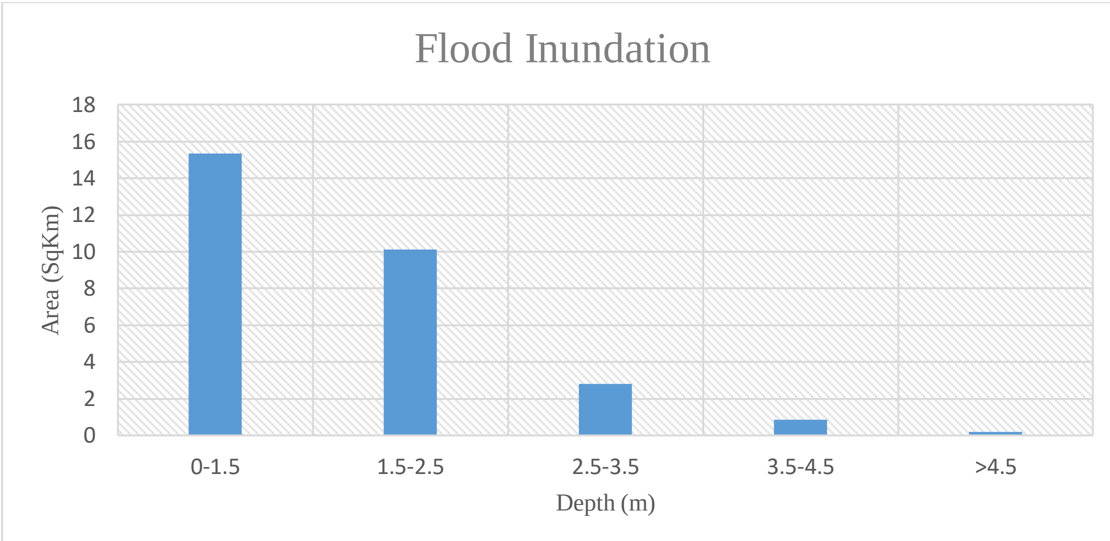

Figure 19 Depth of flooded Area for 100 year return period

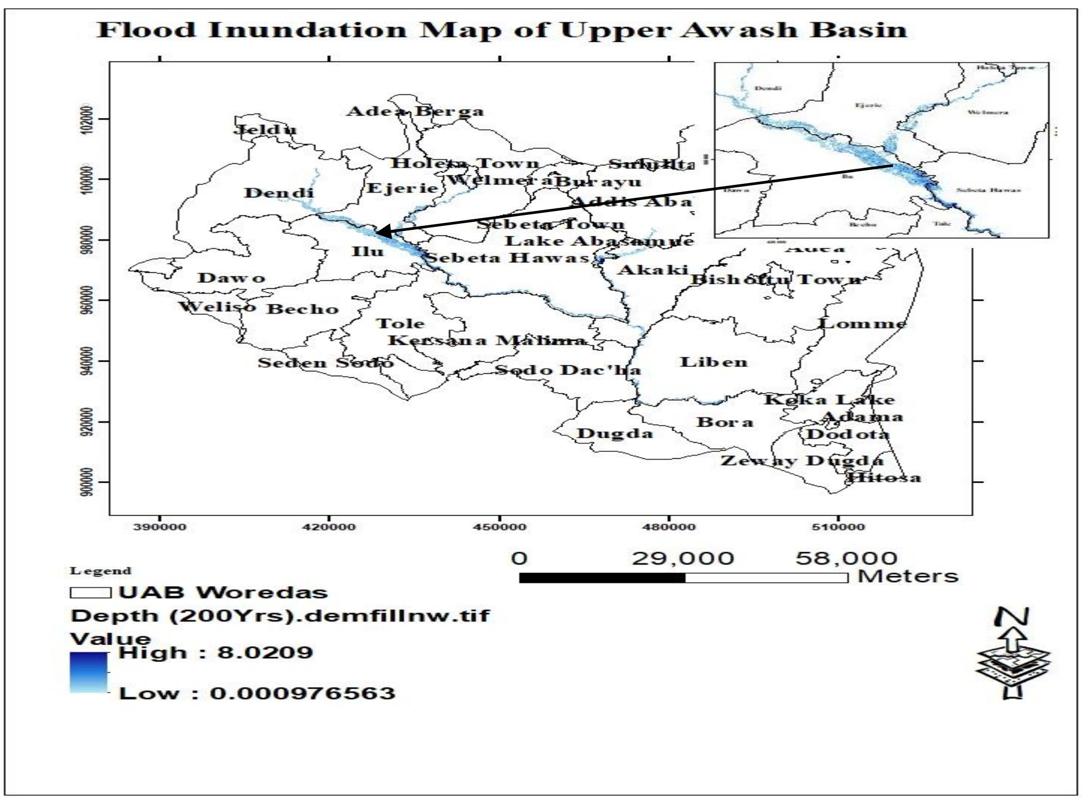

Figure 20 flood depth map for 200 year return periods

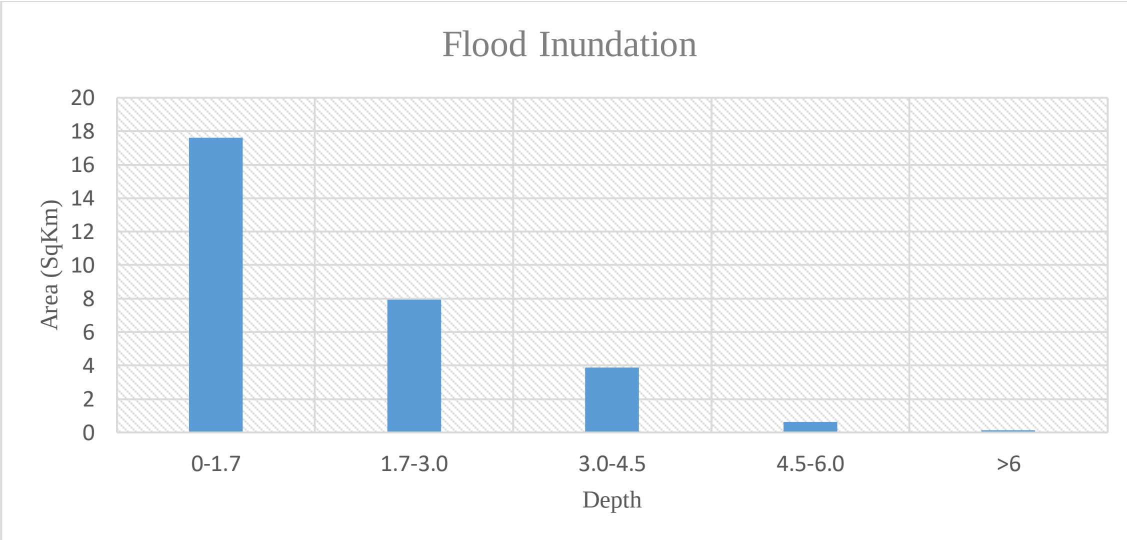

Figure 21 Depth of flooded Area for 200 year return period

Some GPS points were collected during the field survey along the inundated area and this GPS data has been used for the purpose of validation of the flood inundation extent map prepared by using Hec-RAS/Hec-GeoRAS.

5.4 Flood Vulnerability Analysis

Vulnerability analysis which has been carried out for the return period 50, 100, and 200 years indicate that Agriculture land is more vulnerable to flooding than other Land use types in the upper Awash Basin with a total area of 92.09% , 92.15% and 92.18% respectively. The next higher vulnerable land use type for the respective return period is Built up-Area with a total area of 3.34% , 3.33% and 3.31% of total inundated area. From the vulnerability analysis it is observed that the least inundated area for 50, 100, and 200 years return period is 0.04% for all return periods. The detail analysis for Land use vulnerability with different level of vulnerability is give in Table 22, Table 23 and Table 24 for return period of 50, 100, and 200 years return period respectively.

From detail analysis of Agricultural Land vulnerability for different hazard level for the return period of 50 years it observed that 74.36% falls under very low flood hazard level and 15.49%, 6.8% , 2.64% and 0.72% of flooded agriculture land falls under Low, Moderate, High and Very high hazard levels. Whereas flood hazard level for the return period of 100 and 200 depict that 51.45%, 35.44%, 9.731%, 2.77% and 0.62% of the flooded Agricultural Land falls under very low, low, moderate, high and very high and 57.53%, 26.96%, 13.10%, 1.94% and 0.46% of inundated area shows a flood hazard level of very low, low, moderate, high and very high respectively. The Area of vulnerability analysis for agricultural land falling under very low hazard level decreases as the return period increases, on the other hand as the return period increases the flood hazard level falling under very high also decreases. The vulnerability result for the return period of 50, 100 and 200 years are shown in the following figure 25, figure 26 and figure 27 respectively.

From the result of land use vulnerability it is observed that Forest area takes the lowest coverage from all kind of Land use land cover class for the return period of 50, 100, and 200 with the area 0.04, 0.04 and 1.27 hectares respectively as shown on table 22, table 23 and table 24.

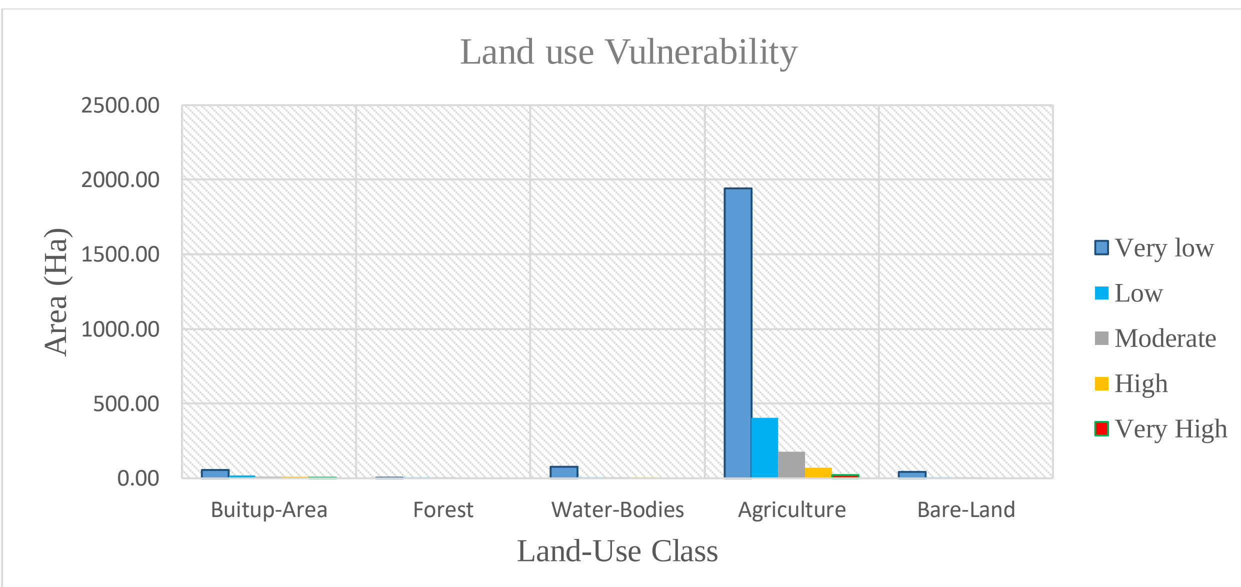

Figure 22 Inundation level of Land Use Class for 50 year return period

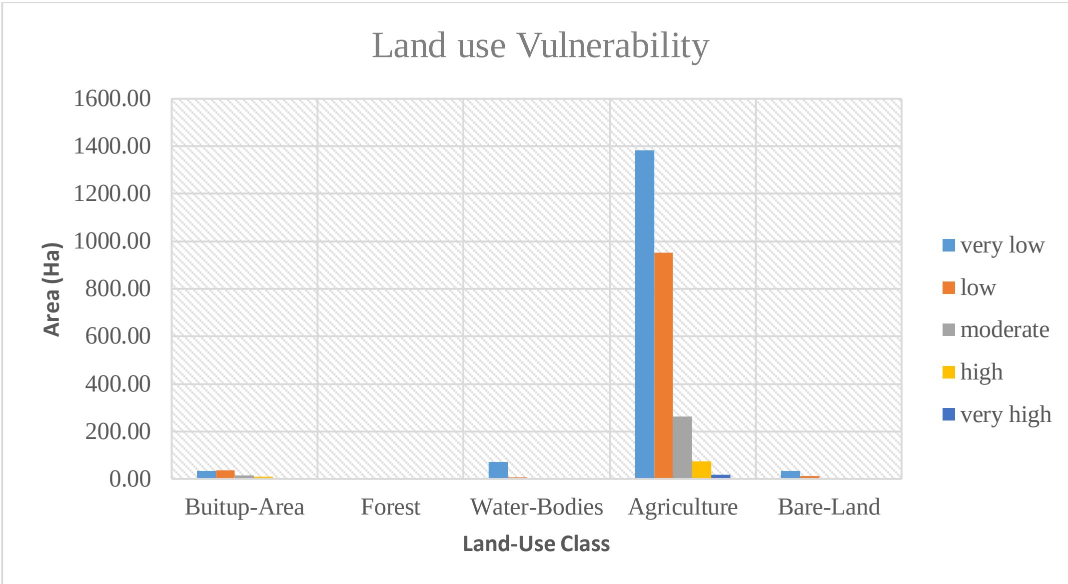

Figure 23 Inundation level of Land Use Class for 100 year return period

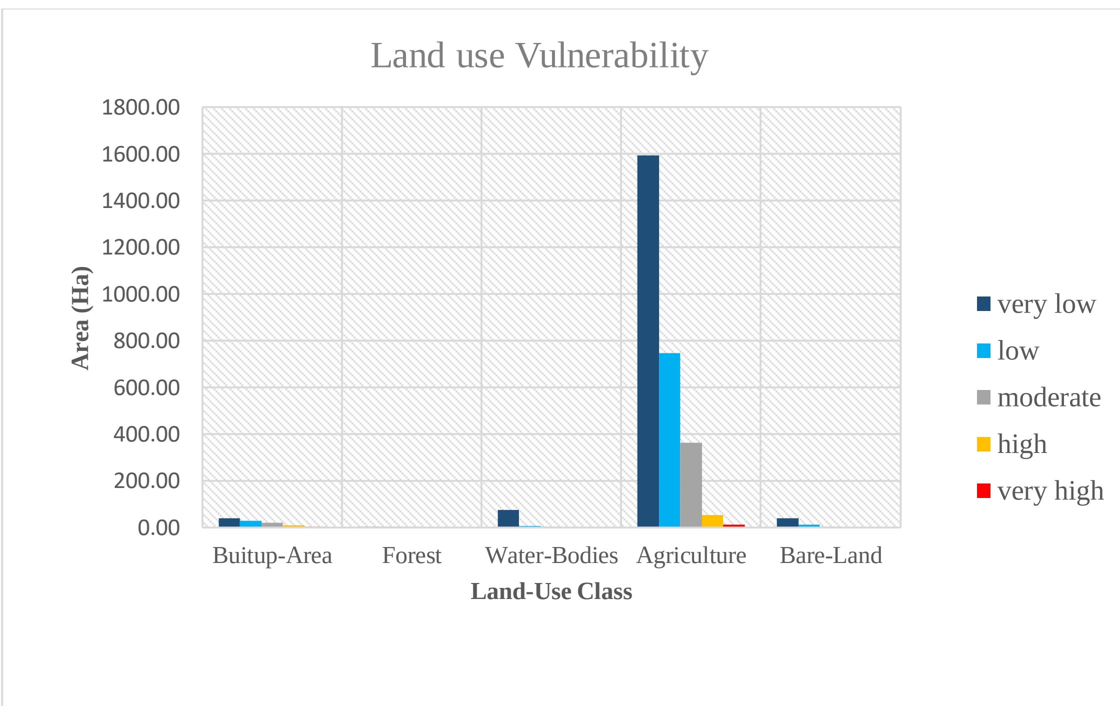

Figure 24 Inundation level of Land Use Class for 200 year return period

CHAPTER SIX

CONCLUSION AND RECOMMENDATION

6.1 CONCLUSION

Flooding in Upper Awash causes a considerable damage to life and property. The damage is more pronounced in Agricultural Land which is a large coverage of the study area and people living in the surrounding area of Awash River. The damage is mainly caused during the rainy season of the country.

The decision factors identified are rainfall, population Density, distance to active channel, landuse land cover, slope of the area, Elevation, drainage density and Soil of the study area. Thematic maps for each factors were prepared using several image processing techniques and GIS operation at different scale. Each of the thematic layers (Classified data sets) were brought to same scale.

Analytical Hierarchy Process (AHP) is multi criteria decision making techniques which provide a systematic approach for assessing and integrating the impacts of various parameters, involving several level of dependent and independent, qualitative as well as quantitative information. The weightage has been assigned taking into the consideration the flood hazard and vulnerability potential of the area, which ultimately lead to the risk zonation. Using ARC-GIS model builder, Overlay analysis of all the thematic layers was carried out to generate separate Flood hazard Map, Flood Vulnerability map and their combination to produce final risk map. The point to be considered during overlay analysis is that all the thematic layers should have discrete values rather than continuous values for assigning weightage. The format of the thematic layers should be in GRID to suit the current framework of AHP analysis.

This study also presents a systematic approach in the preparation of flood risk map with the application of steady flow model in HEC-RAS/HEC-GeoRAS. The major tools/models used in this method is one-dimensional numerical model HEC-RAS and ArcGIS for spatial data processing and HEC-GeoRAS for interfacing between HEC-RAS and ArcGIS.

The assessment of the flood Risk due to the flooding was made with regard to element at risk which area the land use pattern in the flood areas and population density per Sq. Km with integration of flood hazard analysis of the study area. The assessment of the flood risk assessment indicates that a large percentage (more than 84 %) of vulnerable area lies in flood plain area i.e. agricultural land followed by barren land and built up area 10.6% and 1.36% respectively.

Flood hazard map and inundation model were validated using GPS data collected in the field for places with Flood inundation. The results are satisfactory and it validates the logic followed in the analysis and the model developed. It has been observed that in Hazard map the dominant factor is slope followed by distance to river, drainage density, Rainfall, Elevation, soil and LULC, which ultimately contribute to the flooding of the study area. Population density and Land use Land cover is considered as contributing factor to the vulnerability of the study area. Hence, the final risk map generated by combining all the dominant factors as well as the contributing factors to flood risk.

Thus, it has been concluded that the approach used in this thesis is very much useful in delineating the flood hazard map, the flood vulnerability map and ultimately to the flood risk map in the Upper Awash basin. Some of the important conclusions drawn as follow:

- The use of spatial –AHP has been used in the flood hazard mapping and it has been further elaborated with other datasets to generate risk map with more precision.
- Selection of best distribution which is helpful for prediction of future flood event plays an important role.
- Inundation map result for different return period shows that as the return period increases the inundated area due to flooding also increases.
- It has been observed that some of the areas are not inundated but the flood risk assessment indicates there is high risk due to the population factor.

- ❖ Flood risk map has been classified on the basis on the dominance of the different factors and risk is evaluated, it has considered the population and the land use land cover as priority as these are more important while considering the risk of the area. 100

6.2 Recommendation

This study was conducted under major constraint of limited data availability. Therefore, the following recommendations are made for the further studies in the future.

- ❖ The results from the flood hazard map and the risk map suggest flooding in the upper awash basin is recommended as important strategies for flood management.
- ❖ Access to information on flood inundation, prediction, and risk assessment is important and should be made readily available to concerned bodies.
- ❖ It is also recommended Future studies on the flood hazard and risk mapping need to consider the assessment of infrastructure and economic activities since an accurate and detailed risk map is obtained from such data input.
- ❖ This thesis uses a discharge data of 25 years (1988-2012) but future studies needs to take recent data into consideration which may give a good result.
- ❖ It is also recommended future flood risk assessment studies to consider recent population data which is one of the most important factor for risk assessment in the study area.
- ❖ The flood risk management strategies should be made clear and most importantly will need further development.

Reference

Abebe, F. 2007. Flood Hazard Assessment using GIS in Becho plain, Upper Awash Valley, south west of Addis Ababa. MSc Thesis Addis Ababa University, Ethioopia. pp 74

Bernard, E. 2017. The application of GIS in Mapping of designated flood hazard and assessing Risk in Kumasi, Ghana. American scientific research journal for Engineering, Technology and Science. Vol 19. ISSN (Print) 2313-4410 & ISSN (Online) 2313-4402.

Bettina, M., and Virginia, M., (2013). Floods in the WHO European Region: health effects and their prevention.

Daniel A. 2007 Assessment of flood risk in Dire Dawa Town, Eastern Ethiopia, Using GIS. MSc Thesis Addis Ababa University, Ethiopia. pp 96

Cameron T. Ackerman, Hydrologic Engineering Center (HEC). (2011). GIS Tools for support of HEC-RAS using ArcGIS: *Reference manual*, U.S Army corps of Engineers,

Destaye, G. 2009. Application of GIS and Remote Sensing for flood hazard and Risk Analysis: in the case of Boyo Catchment. MSc Thesis Addis Ababa University. Ethiopia.

Emmanuel, O.,(2013). Application of Remote Sensing and Geographical Information Systems in Flood Management: A Review. Research Journal of Applied Sciences, Engineering and Technology 6(10): 1884-1894.

Eric, F. (2011). Flood hazard mapping using Aster image data with GIS", International Journal of Geomatics and Geosciences, Volume 1, No 4, ISSN 0976 – 4380

Fosu, C., Forkuo, Eric K. and Asare, M. Y., (2012). River Inundation and Hazard Mapping – a Case Study of Susan River – Kumasi. Proceedings of Global Geospatial Conference 2012,Québec City, Canada,

Harlan H. Bengtson, PhD, P.E. 2002. Frequency Analysis of Flood Data, U.S. Department of Transportation. Hydraulic Design Series No. 2, Second Edition.

Kafle, T.P., Hazarika, M.K., and Samarakoon, L., (2007) "Flood risk assessment in the flood Plain of Bagmati River in Nepal". ACRS.

Karagiozi, E., Fountoulis, I., Konstantinidis, A., Andreadakis, E., Ntouros, K., (2011) "Flood Hazard Assessment based on Geomorphological Analysis with GIS tools - The Case of Laconia Peloponnesus, Greece. GIS Ostrava,.

Kefyalew A.,2003. Integrated Flood Management: Case study Ethiopia, Water Resource Consultant, Ethiopia.

Kebede, B. 2012. Application of GIS and Remote Sensing Techniques for Flood Hazard and Risk Assessment: The Case of Dugeda Bora Woreda of Oromiya Regional State, Ethiopia. *Paper for the 2012 Berlin Conference on the Human Dimensions of Global Environmental Change.*

Muhammed, Q. 2018.Flood Inundation Modeling of River Kabul using HEC-GEORAS, conference paper. https://www.researchgate.net/publication/324168722.

Nippon Koei. 1996. Feasibility study on the Becho plain agricultural development project. Final report. Volume II, Annex I and II.

Nirman, B. 2017. Flood Frequency Analysis Using Gumbel's Distribution Method: A Case Study of Lower Mahi Basin, India. *Journal of Water Resources and Ocean Science*.doi: 10.11648/ j.wros.20170604.11 Vol. 6, No. 4, pp. 51-54.

Ologunorisa, E. 2004. An Assessment of Flood vunerabilityzone in the Niger Delta, Nigeria. International Journal of Environmental Studies, Vol. 61(1), pp. 31-38.

Prasoon, S., and Ayushi V.,(2016). Identification of flood risk on urban road network using Hydrodynamic Model Case study of Mumbai floods. New Delhi: The Energy and Resources Institute. 105 pp.

Roger, F., Mike A., Franziska M., and Sari K., (2004). Floods, health and climate change: a strategic review.

Sanyal, J. and Lu X., (2006). GIS-based flood hazard mapping at different administrative scales: A case study in Gangetic West Bengal, India. Department of Geography, National University of Singapore, Singapore. doi:10.1111/j.1467-9493.2006.00254.x

Saaty, T. L, 1980. The Analytic Hierarchy Process, New York: McGraw Hill.

Shielis, B. 2004. Stream Flow simulation for the upper Awash river basin, Addis Ababa University, Ethiopia. pp 110

Shook, G. 1997. An assessment of disaster risk and its management in Thailand.pp 128

Simonovic, Slobdan.P., (2009). A new method for spatial and temporal analysis of risk in water resources management. Journal of Hydro informatics.

Singh, A. K., Sharma, A. K., (2009). “GIS and a Remote Sensing Based Approach for Urban Flood-Plain Mapping for The Tapi Catchment, India”, Journal of Hydrological Sciences.

Somaiyeh, K., Mehran, M., Sorayya, K., (2015). Integrated application of HEC-RAS and GIS and RS for flood risk assessment in Lighvan Chai River. *International Journal of Engineering Science Invention. ISSN (Online): 2319 – 6734,Vol 4 Issue 4. PP.38-45*

Sravani, D., Balaji, N., (2013). Flood Inundation Mapping of Thamiraparani River Basin Using HECGeo RAS and SWAT. International Journal of Engineering Research & Technology (IJERT) ISSN: 2278-0181 Vol. 2 Issue 7,

Thielen, J., Bartholmes, J., Ramos, H., and de Roo, A.,(2009). The European Flood Alert System Part 1: Concept and development. Hydrol. Earth Syst. Sci., 13, 125–140.

Water Resources Development Authority. 1983. Geology Report, Becho plains Flood Control and Drainage Project.

Yirga, K. (2016). Flood Hazard and Risk Assessment Using GIS and Remote Sensing in Lower Awash Sub-basin, Ethiopia. Journal of Environment and Earth Science, Vol.6, No.9, ISSN 2224-3216 (Paper) ISSN 2225-0948 (Online)

Yitae, S. 2015. Impact of climate change on hydrology of upper Awash Basin (Ethiopia):Inter-comparison of old SRES and new RCP scenarios, conference paper. https://www.researchgate.net/publication/316505332

Yitae, S., Sintayehu, L. (2015). Flood Hazard assessment and Mapping of flood inundation area of Awash River Basin in Ethiopia Using GIS and HEC-GeoRAS/HEC-RAS Model. DOI: 10.4172/2165-784X.1000179

Zelalem A. 2011. Flood Mapping and Modeling on Fogera Flood Plain: A Case Study on Ribb River. Addis Ababa University, Ethiopia pp 93

Zhang, J., Tomoharu, H., Zhang, C., Matsumoto, T., (2003), "GIS and flood inundation model-based flood risk assessment in urbanized floodplain". GIS and RS in Hydrology, Water Resources and Environment, **1**, pp 128

APPEDIX I. GPS Data

SN	X	Y	SN	X	Y	SN	X	Y
1	444882	979028	89	474374	955283	177	415003	990028
2	441854	980345	90	474660	954132	178	414835	991755
3	438932	982398	91	474659	952693	179	507952	958002
4	436684	980983	92	474715	950506	180	507893	957173
5	439137	980139	93	475458	948779	181	508443	957509
6	441433	980989	94	474140	946881	182	508599	958258
7	442646	978907	95	472936	945961	183	509188	958140
8	433361	978505	96	472652	948723	184	509227	957647
9	431808	977832	97	471214	939517	185	510150	957529
10	438530	976365	98	490865	947680	186	509875	958061
11	432011	975465	99	492011	948715	187	511249	956819
12	431077	973777	100	493901	946701	188	510915	955814
13	428519	975393	101	495046	947622	189	511680	956386
14	429137	973338	102	495734	944629	190	511818	953527
15	426727	970872	103	494989	942960	191	512290	952856
16	426156	969755	104	455845	981220	192	512878	953093
17	429221	976978	105	456288	980563	193	512878	952620
18	427357	976123	106	457411	980456	194	513193	949347
19	431205	973100	107	458013	981690	195	513743	949939
20	427500	969518	108	457357	978960	196	514469	949939
21	426154	968533	109	458741	978696	197	515038	949900
22	417076	974078	110	457878	977462	198	514390	949308
23	426424	980602	111	469944	976743	199	513802	949268
24	432648	982013	112	468011	976429	200	513252	948618
25	424341	959535	113	467723	975563	201	512448	948617
26	424051	954515	114	468507	975221	202	499633	943134
27	419835	950857	115	467540	974434	203	501125	943213
28	418194	944599	116	467983	973488	204	502027	943253
29	424479	942557	117	454612	975838	205	502498	943884
30	427244	950731	118	455342	975102	206	503912	942740
31	437808	957989	119	455498	974340	207	500693	942306
32	456100	954075	120	454609	973763	208	499476	941675
33	459859	951984	121	454034	972924	209	417462	970492
34	461032	945948	122	453120	973003	210	428171	964477
35	460188	944144	123	453774	974000	211	429704	965122
36	460425	957567	124	454298	975208	212	432521	962930

37	458297	961968	125	453253	975787	213	455590	976914
38	456338	967159	126	453281	977257	214	479851	990181
39	469119	974104	127	448756	983525	215	479849	987346
40	472841	975828	128	447611	982894	216	478399	986294
41	476847	975077	129	446636	981859	217	478720	984349
42	479024	977148	130	446291	980651	218	479607	986131
43	478739	980255	131	413231	990722	219	481621	986940
44	472443	980259	132	412655	988997	220	481139	990424
45	480859	986124	133	411736	987445	221	480414	989209
46	504609	973978	134	410872	985087	222	443962	993150
47	502376	974208	135	411095	982209	223	443168	991852
48	498885	972136	136	413442	982376	224	442167	990722
49	496080	972654	137	413505	985024	225	440708	990180
50	492702	971849	138	414198	988015	226	440375	990725
51	441500	990807	139	433003	959285	227	435904	970994
52	442085	991560	140	430502	957854	228	435575	972087
53	442503	992691	141	432997	956057	229	435009	973085
54	443046	993780	142	435141	957130	230	433637	971710
55	437084	990856	143	436454	959878	231	432311	969480
56	434915	989769	144	439310	960352	232	431080	968295
57	433247	988473	145	442524	961662	233	407994	960730
58	431700	985668	146	442164	959630	234	412522	961005
59	430320	982737	147	444547	962377	235	409699	964139
60	431739	984076	148	444313	965008	236	414510	964129
61	432491	984954	149	480655	984582	237	418475	965828
62	433118	986462	150	475859	983212	238	413954	968965
63	433912	987550	151	474703	982156	239	409970	958451
64	436499	989641	152	474142	980573	240	455399	986397
65	450204	987443	153	476208	980923	241	450029	970453
66	452536	985890	154	477223	980360	242	448184	968793
67	450501	991759	155	475822	979269	243	446152	968035
68	450379	993812	156	474491	978883	244	448044	969743
69	448420	993689	157	473196	979130	245	448045	971167
70	449961	992891	158	471305	977407	246	432823	965205
71	496776	931922	159	471095	978216	247	433628	966059
72	494800	931010	160	471861	972267	248	434198	968053
73	493144	929616	161	471058	974908	249	434719	968622
74	495654	928811	162	483244	981202	250	435004	969856

75	**497096**	**930849**	**163**	**485414**	**980180**	**251**	**483426**	**963089**
76	**498164**	**932243**	**164**	**482823**	**978456**	**252**	**484308**	**962819**
77	**466337**	**979810**	**165**	**484890**	**981553**	**253**	**484462**	**964399**
78	**468561**	**980502**	**166**	**483664**	**979934**	**254**	**485039**	**967599**
79	**468256**	**982893**	**167**	**483280**	**982222**	**255**	**486727**	**968138**
80	**468525**	**984165**	**168**	**482579**	**980251**	**256**	**487532**	**968523**
81	**464419**	**979735**	**169**	**481878**	**979125**	**257**	**488644**	**968523**
82	**464690**	**982279**	**170**	**482788**	**979477**	**258**	**488415**	**970180**
83	**444599**	**981183**	**171**	**483909**	**981905**	**259**	**487955**	**970990**
84	**448310**	**974740**	**172**	**487839**	**967713**	**260**	**436197**	**977405**
85	**452812**	**988343**	**173**	**485729**	**967136**	**261**	**448285**	**973779**
86	**450820**	**989734**	**174**	**486611**	**966210**	**262**	**448141**	**972212**
87	**440109**	**978298**	**175**	**487033**	**967212**	**263**	**449842**	**972020**
88	**484003**	**966173**	**176**	**483695**	**964708**	**264**	**488260**	**967212**
						265	**485038**	**965979**

APPENDIX II. Maximum Discharge data for different Gauging Station (m^3/s)

Awash Belo GS		Melka Kunture GS		Addis Alem GS		Ombole GS		Akaki GS	
Year	**Max (Q)**	**Year**	**Max (Q)**	**Year**	**Max (Q)**	**Year**	**Max (Q)**	**Year**	**Max (Q)**
1988	37.84	1988	365.493	1988	115.168	1988	674.8	1988	338.97
1989	37.84	1989	169.851	1996	113.038	1989	536.5	1989	347.67
1990	36.389	1990	169.851	2012	81.388	1990	427.5	1990	421.85
1991	37.84	1991	225.398	2009	81.134	1991	566.1	1991	298.52
1992	38.361	1992	186.504	1999	70.419	1992	347.7	1992	272.47
1993	35.157	1993	307.421	2010	67.341	1993	526.1	1993	381.25
1994	38.466	1994	180.862	1998	64.274	1994	377.9	1994	412.88
1995	32.929	1995	167.155	2008	63.665	1995	286.2	1995	372.21
1996	39.516	1996	398.626	2007	62.144	1996	803.1	1996	252.25
1997	35.157	1997	163.154	2001	49.153	1997	244.4	1997	321.25
1998	49.51	1998	347.518	1993	48.482	1998	632.3	1998	402.25
1999	45.867	1999	289.232	2002	48.363	1999	659.582	1999	450.25
2000	49.863	2000	164.06	1990	46.758	2000	313.332	2000	255.78
2001	41.62	2001	264.853	1995	44.426	2001	494.041	2001	435.34
2002	36.54	2002	271.477	2003	44.123	2002	302.866	2002	219.87
2003	47.241	2003	271.477	2006	40.813	2003	339.754	2003	420.06
2004	48.283	2004	235.233	1997	39.861	2004	230.229	2004	250.47
2005	48.283	2005	320.639	2005	35.723	2005	415.028	2005	266.85
2006	45.52	2006	458.148	2011	33.648	2006	421.188	2006	236.37
2007	50.039	2007	452.076	2004	33.167	2007	382.066	2007	356.89
2008	52.904	2008	458.148	1992	32.079	2008	360.474	2008	223.3
2009	51.284	2009	555.178	1989	28.865	2009	462.484	2009	267.87
2010	56.576	2010	291.944	2000	28.634	2010	374.789	2010	241.14
2011	51.463	2011	422.44	1994	26.915	2011	462.484	2011	358.1
2012	51.822	2012	476.66	1991	20.294	2012	478.952	2012	354.48

APPENDIX III. Woreda's Flood Hazard and Flood Risk Detail

A. Area in of woredas Under differet Flood Hazard level (m^2)

SN	Woreda Name	Hazard Level				
		Very low	Low	Moderate	High	Very high
1	Jeldu	3082656.25	28441718.75	18392500	7427812.5	0
2	Dendi	37415156.3	118089062.5	142383906.3	164990781	223325313
3	Ejerie	5854687.5	34379843.75	55743437.5	98745937.5	201829219
4	Welmera	51214843.8	99016875	134736406.3	172307344	112377813
5	Adea Berga	3652656.25	5935937.5	5422500	8078750	3732031.25
6	Holeta Town	0	204843.75	1990781.25	11307968.8	4342812.5
7	Bereh	91446718.8	111372500	210873125	106552969	9536406.25
8	Sulullta	5452656.25	5110000	502656.25	47500	0
9	Adama	7995468.75	11508125	11587187.5	6761718.75	0
10	Lomme	16785781.3	87488281.25	172981562.5	172749375	4721250
11	Gimbichu	19137187.5	139722500	144875312.5	5997656.25	0
12	Adea	71714843.8	199640468.8	297644375	242777188	82663281.3
13	Dugda	8336250	44716562.5	128178125	100096406	2145156.25
14	Bishoftu Town	900156.25	3988437.5	6950156.25	16347031.3	11839218.8
15	Bora	4006250	46305312.5	147085468.8	178635469	15008750
16	Liben	53061250	101570625	204739218.8	262506250	81676093.8
17	Akaki	34562968.8	89299843.75	197838593.8	194416250	65962500
18	Dodota	30380312.5	56564531.25	67066875	11315468.8	0
19	Zeway Dugda	28908281.3	47517500	49489687.5	7645312.5	0
20	Hitosa	9042656.25	28172656.25	4612812.5	0	0
21	Weliso	0	4488750	15867343.75	45807500	17834375
22	Dawo	1099531.25	26266718.75	48386875	107615625	290000313
23	Ilu	0	0	316406.25	26909687.5	283290469
24	Sebeta Hawas	58022500	99445312.5	232825937.5	264055000	213269844
25	Kersana Malima	63791562.5	137971718.8	172055625	131806406	51520468.8
26	Tole	22635312.5	51109687.5	54118750	130500313	162365000
27	Becho	611875	15446093.75	27702656.25	169177031	217045781
28	Seden Sodo	8770937.5	15519375	37600000	75897968.8	16119531.3
29	Sodo Dac'ha	31279687.5	107685937.5	127772500	86690156.3	38980000
30	Sebeta Town	112968.75	652031.25	3940000	2601406.25	104062.5
31	Burayu	8003906.25	8822656.25	26870156.25	40909375	0
32	Addis Ababa	32581718.8	75048750	131742500	202835781	70511250

B. Area of woredas under different Risk level in (m^2)

SN	W_NAME	Risk Level				
		VERY_LOW	LOW	MODERATE	HIGH	VERY_HIGH
1	Jeldu	2621406.25	20472812.5	21316093.75	10840469	2037343.8
2	Dendi	84239062.5	142021719	193816250	250726563	15173594
3	Ejerie	22108750	45038125	87074843.75	212406719	29904219
4	Welmera	94264687.5	111427031	158145625	167735781	38080156
5	Adea Berga	3380468.75	5222031.25	5578281.25	8020625	4620468.8
6	Holeta Town	24687.5	1093906.25	7993437.5	4546718.8	4187656.3
7	Bereh	174760000	173525156	148694375	30009063	2773750
8	Sulullta	3460781.25	5102500	2279687.5	226093.75	39218.75
9	Adama	7823593.75	11303125	11608750	6662500	441875
10	Lomme	95383750	167135156	168247812.5	23581719	371406.25
11	Gimbichu	147757188	141154219	20385000	436250	0
12	Adea	252717031	291919219	238582812.5	101001875	10191563
13	Dugda	51894218.8	125452500	102118125	3085625	1718.75
14	Bishoftu Town	633281.25	3390781.25	5875312.5	13267656	16857031
15	Bora	46323125	144466719	179107656.3	20445469	298750
16	Liben	137205000	201055938	267762187.5	92431719	5098593.8
17	Akaki	115088594	189049844	193457031.3	75855313	8600468.8
18	Dodota	82543593.8	65681406.3	15907500	1186718.8	0
19	Zeway Dugda	28922500	90027968.8	13237968.75	867187.5	0
20	Hitosa	9355000	27595156.3	4726875	45312.5	0
21	Weliso	175625	14308593.8	38550156.25	12882188	17735938
22	Dawo	10453437.5	40576093.8	97773125	293151250	31415156
23	Ilu	0	301718.75	26197500	275491875	8525468.8
24	Sebeta Hawas	125206563	226215781	275225937.5	227322656	13641094
25	Kersana Malima	126418438	199220313	160907812.5	66796563	3801718.8
26	Tole	44356875	68044687.5	133223437.5	163066563	12037500
27	Becho	7661875	27676406.3	162651250	221600156	10257656
28	Seden Sodo	14665937.5	35653906.3	75542343.75	25697813	2088437.5
29	Sodo Dac'ha	120568438	132435781	94350000	42701094	2302031.3
30	Sebeta Town	52500	390312.5	2476562.5	3103906.3	1387187.5
31	Burayu	9830000	16929218.8	31718750	26116875	156.25
32	Addis Ababa	24794375	52333750	104493281.3	165051406	165987500

APPENXIX III Accuracy Assessment Detail

Prediction	Builtup_Area	Water_Bodies	Forest	Agriculture	Barren_Land	Ground Truth
Builtup_Area	46	0	0	0	1	47
Water_Bodies	0	49	0	0	0	49
Forest	0	0	43	0	0	43
Agriculture	4	1	7	48	19	79
Barren_Land	0	0	0	2	30	32
Total	50	50	50	50	50	**250**

Prediction	Builtup_Area	Water_Bodies	Forest	Agriculture	Barren_Land
Builtup_Area	92	0	0	0	2
Water_Bodies	0	98	0	0	0
Forest	0	0	86	0	0
Agriculture	8	2	14	96	38
Barren_Land	0	0	0	4	60
Total					

Comision Error

Builtup_Area	1	47	2.127659574
Water_Bodies	0	49	0
Forest	0	43	0
Agriculture	41	79	51.89873418
Barren_Land	2	32	6.25

Omission Error

Builtup_Area	4	50	8
Water_Bodies	1	50	2
Forest	7	50	14
Agriculture	2	50	4
Barren_Land	20	50	40

Producer Accuracy

Builtup_Area	46	50	92

Water_Bodies	49	50	98
Forest	43	50	86
Agriculture	48	50	96
Barren_Land	30	50	60

Users Accuracy

Builtup_Area	46	47	97.87234043
Water_Bodies	49	49	100
Forest	43	43	100
Agriculture	48	79	60.75949367
Barren_Land	30	32	93.75

Overall Accuracy = 0.864

Kappa Coefficient = 0.83

APPENDIX IV. Pairwise comparison of flood causative factors

	Slope	D/ce-River	Drng dnsty	Rainfall	Elevation	Soil	LULC
Slope	1	2	2	3	2	3	5
D/ce – River	½	1	3	2	2	3	3
Drng dnsty	½	½	1	2	3	3	5
Rainfall	1/3	½	½	1	2	2	3
Elevation	½	½	1/3	1/2	1	3	3
Soil	1/3	1/3	1/3	1/3	1/3	1	2
LULC	1/5	1/3	1/5	1/3	1/3	1/2	1
Total	**3.36**	**5.16**	**7.36**	**9.16**	**10.66**	**15.5**	**22**

Normalized Pairwise Comparison

	Slope	D/ce-River	Drng dnsty	Rainfall	Elevation	Soil	LULC	**Criteria Weight**
Slope	0.30	0.39	0.27	0.33	0.19	0.19	0.23	**0.27**
D/ce – River	0.15	0.19	0.41	0.22	0.19	0.19	0.14	**0.21**
Drng dnsty	0.15	0.10	0.14	0.22	0.28	0.13	0.23	**0.17**
Rainfall	0.10	0.10	0.07	0.11	0.19	0.18	0.14	**0.13**
Elevation	0.15	0.10	0.04	0.05	0.09	0.19	0.14	**0.11**
Soil	0.10	0.06	0.04	0.04	0.03	0.06	0.09	**0.06**
LULC	0.06	0.06	0.03	0.04	0.03	0.03	0.05	**0.05**

Consistency ratio was calculated using the following procedure

Criteria Weight	**0.27**	**0.21**	**0.17**	**0.13**	**0.11**	**0.06**	**0.05**
	Slope	D/ce-River	Drng dnsty	Rainfall	Elevation	Soil	LULC
Slope	1	2	2	3	2	3	5
D/ce -River	½	1	3	2	2	3	3
Drng dnsty	½	½	1	2	3	3	5
Rainfall	1/3	½	½	1	2	2	3
Elevation	½	½	1/3	1/2	1	3	3
Soil	1/3	1/3	1/3	1/3	1/3	1	2
LULC	1/5	1/3	1/5	1/3	1/3	1/2	1

	Slope	D River	Drng dnsty	Rain	Elev	Soil	LULC	**WtSum**	**Crit Wt**	
Slope	0.27	0.42	0.37	0.39	0.22	0.18	0.25	**2.1**	**0.27**	**7.78**
DR	0.14	0.21	0.51	0.26	0.22	0.18	0.15	**1.67**	**0.21**	**7.95**
DD	0.14	0.11	0.17	0.26	0.33	0.18	0.25	**1.44**	**0.17**	**8.47**
Rf	0.09	0.11	0.09	0.13	0.22	0.12	0.15	**0.91**	**0.13**	**7**
Elv	0.14	0.11	0.06	0.06	0.11	0.18	0.15	**0.81**	**0.11**	**7.36**
Soil	0.09	0.07	0.06	0.04	0.04	0.06	0.10	**0.46**	**0.06**	**7.67**
LULC	0.05	0.07	0.03	0.04	0.04	0.03	0.05	**0.31**	**0.05**	**6.2**

Criteria Weight	**0.27**	**0.21**	**0.17**	**0.13**	**0.11**	**0.06**	**0.05**	
	Slope	D/ce-River	Drng dnsty	Rainfall	Elevation	Soil	LULC	**Wtd Sum**
Slope	0.27	0.42	0.37	0.39	0.22	0.18	0.25	**2.1**
D/ce – River	0.14	0.21	0.51	0.26	0.22	0.18	0.15	**1.67**
Drng dnsty	0.14	0.11	0.17	0.26	0.33	0.18	0.25	**1.44**
Rainfall	0.09	0.11	0.09	0.13	0.22	0.12	0.15	**0.91**
Elevation	0.14	0.11	0.06	0.06	0.11	0.18	0.15	**0.81**
Soil	0.09	0.07	0.06	0.04	0.04	0.06	0.10	**0.46**
LULC	0.05	0.07	0.03	0.04	0.04	0.03	0.05	**0.31**

APPENDIX IV. Geological Description

Q	Alluvial and lacustrine deposits:Sand,silt,clay, diatomite,limestone and beach sand.
Qb	Basalt flows,spatter cones and hyaloclastites a) Transitional type between alkaline and tholeiitic. b) Alkaline olivine basalt.
Qr	Rhyolitic volcanic centers,obsidian pitchstone,pumice,ignimbrite,tuff,ubordinate trachytic flows (predominantly peralkaline in composition)
Qd	Dino Formation:Ignimbrite,tuff,course pumice,waterlain pyroclastic rocks with rare intercalations of lacustrine sediments.
NQtb	Bishoftu Formation : Alkaline basalt and trachyte.
Nc	Chilalo Formation(Lower part) : Trachyte,trachy- basalt, peralkaline rhyolite with subordinate akaline. basalt.
Nn	Nazret Series : Ignimbrites,unwelded tuffs,ash flows, rhyolitic flows,domes and trachyte.
Ntb	Tarmaber Megezez Formation : Transitional and alkaline basalt.
PNa	Alage Formation : Transitional and subalkaline basalts with minor rhyolite and trachyte eruptives.

APPENDIX V. Vulnerability of Land Use Land Cover

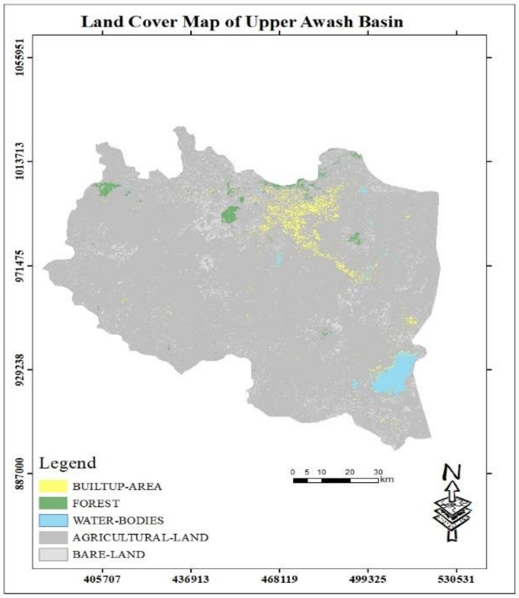

A

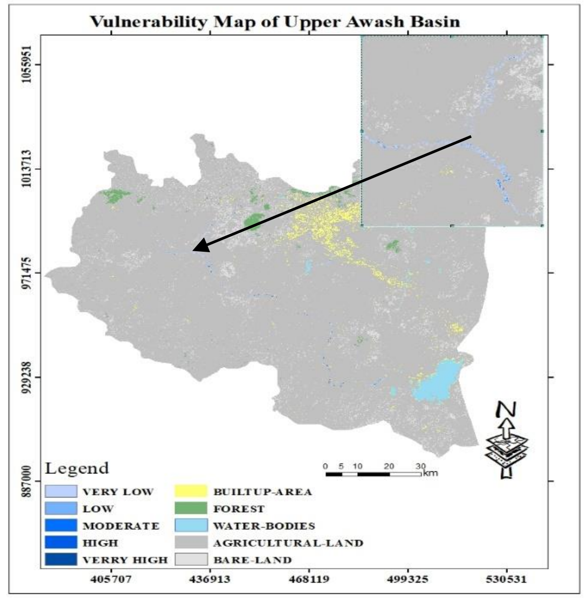

b

c

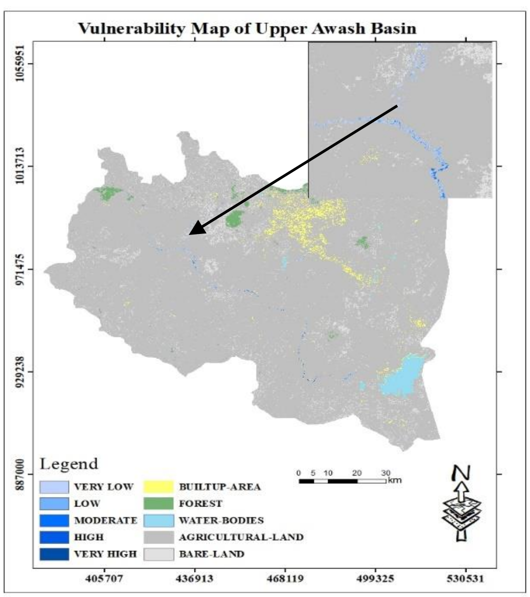

d

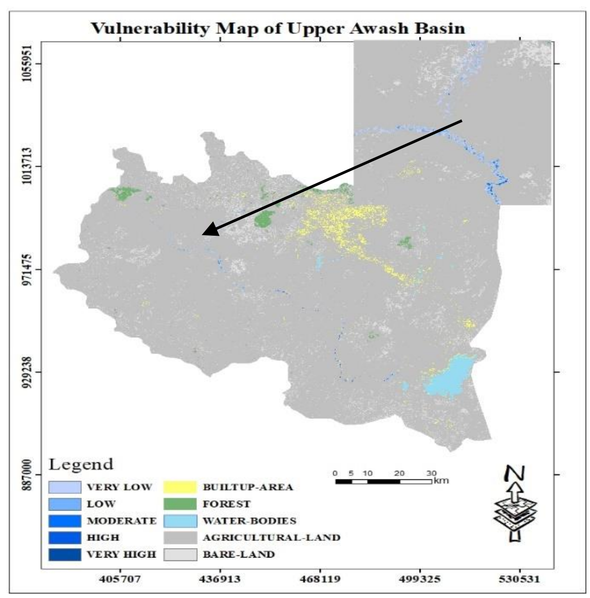

APPENDIX VI. Q-Q plot

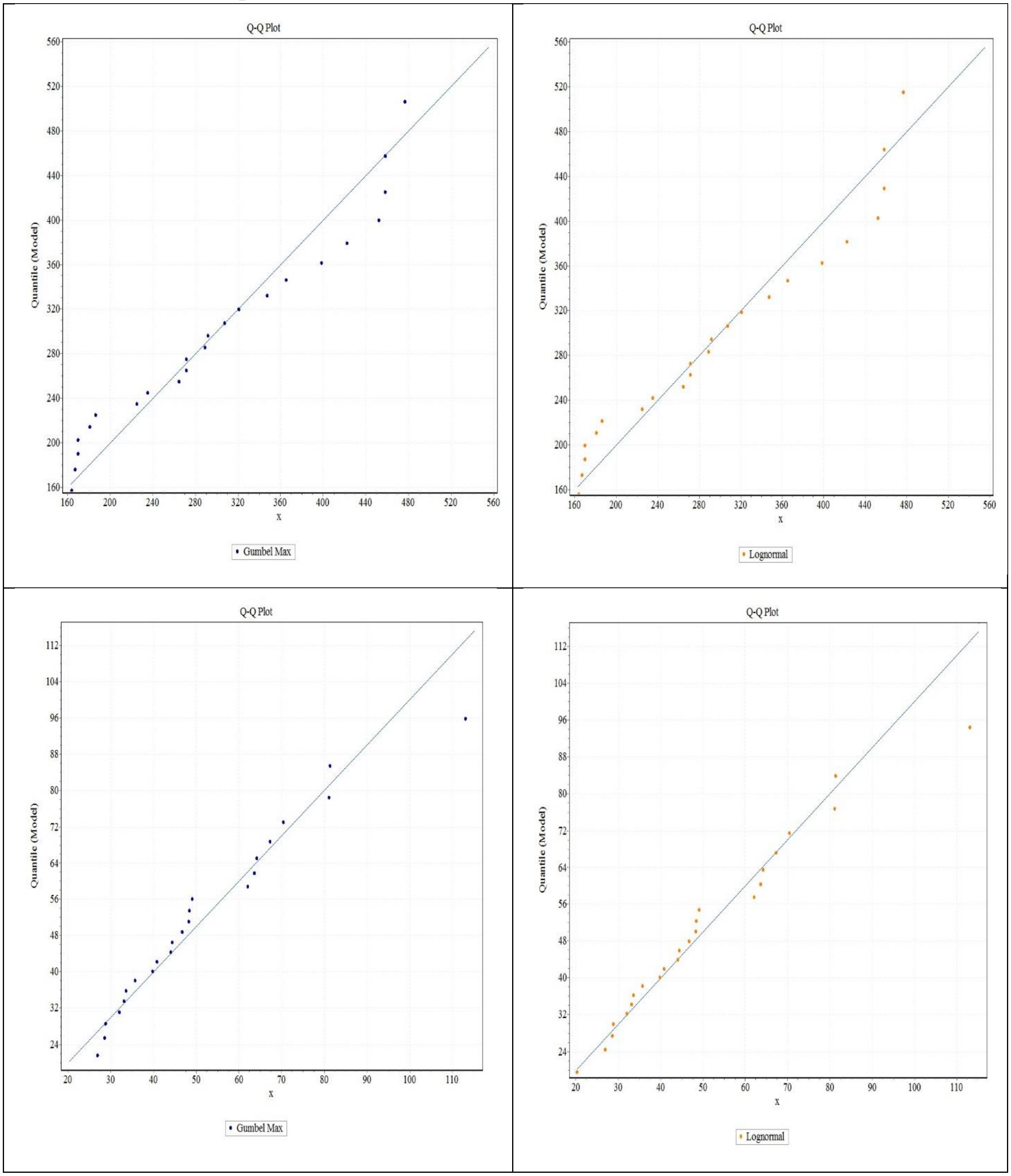

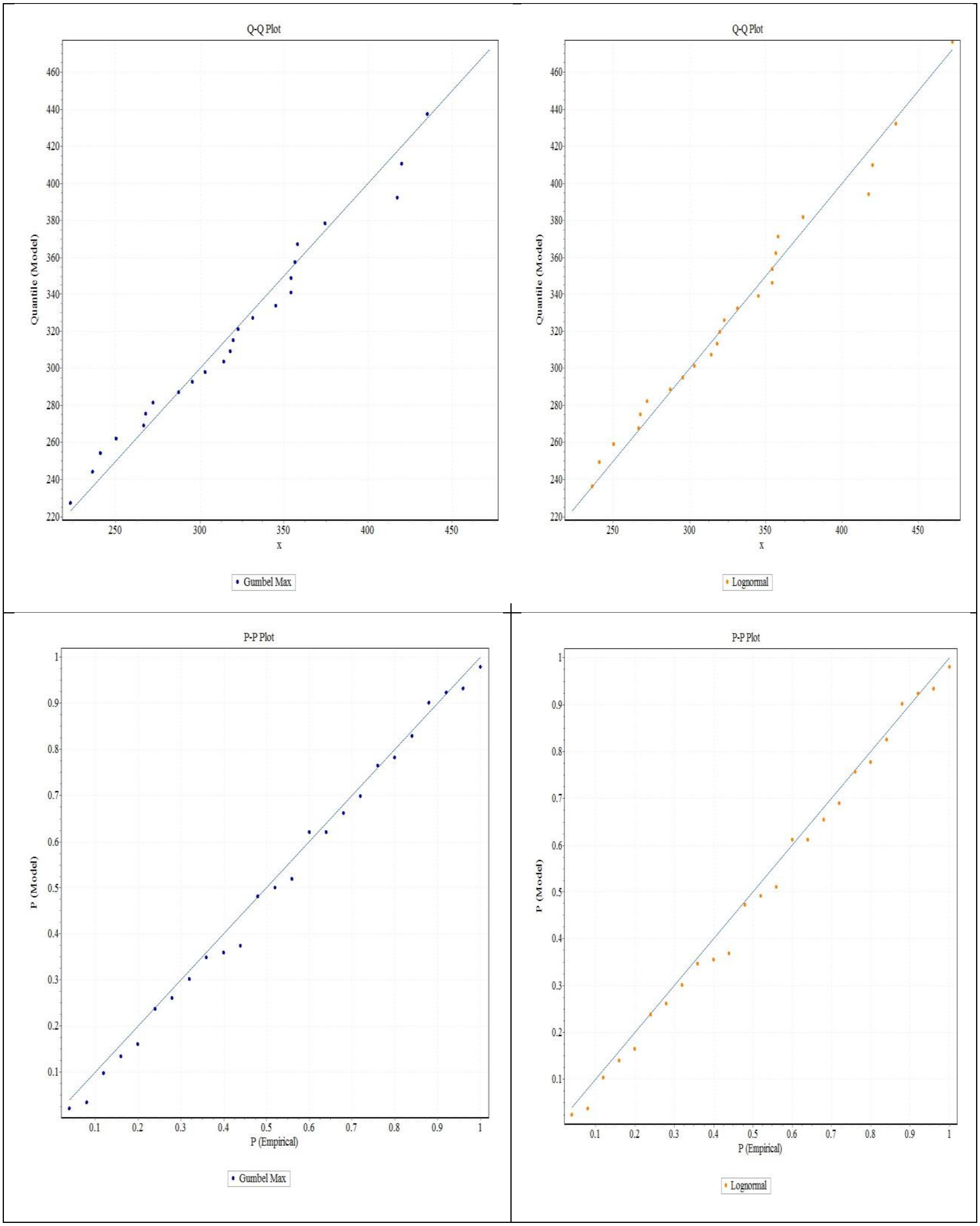
Q-Q Plot
Quantile (Model)
x
Gumbel Max
Q-Q Plot
Quantile (Model)
x
Lognormal
P-P Plot
P (Model)
P (Empirical)
Gumbel Max
P-P Plot
P (Model)
P (Empirical)
Lognormal

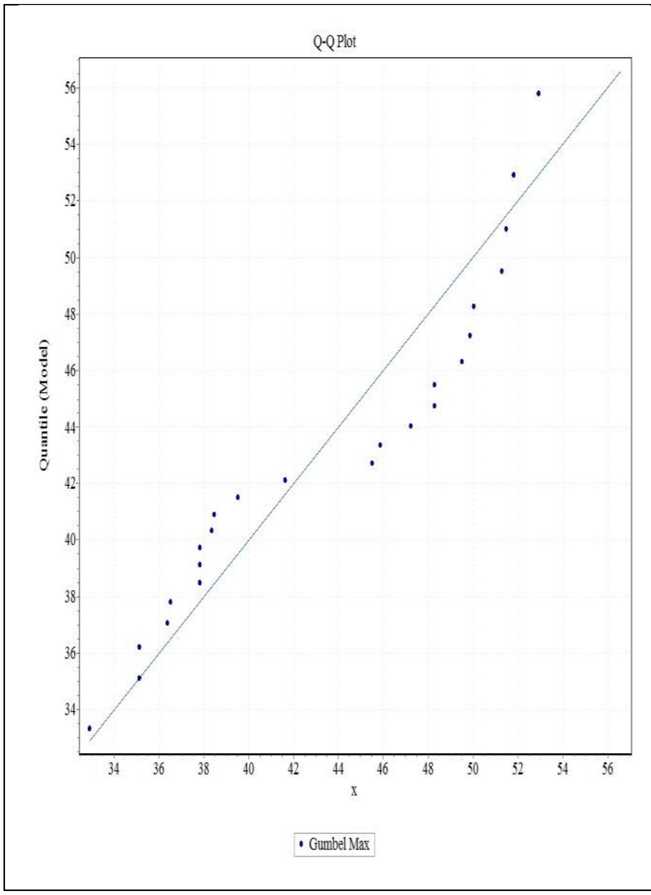
Q-Q Plot
Quantile (Model)
x
Gumbel Max

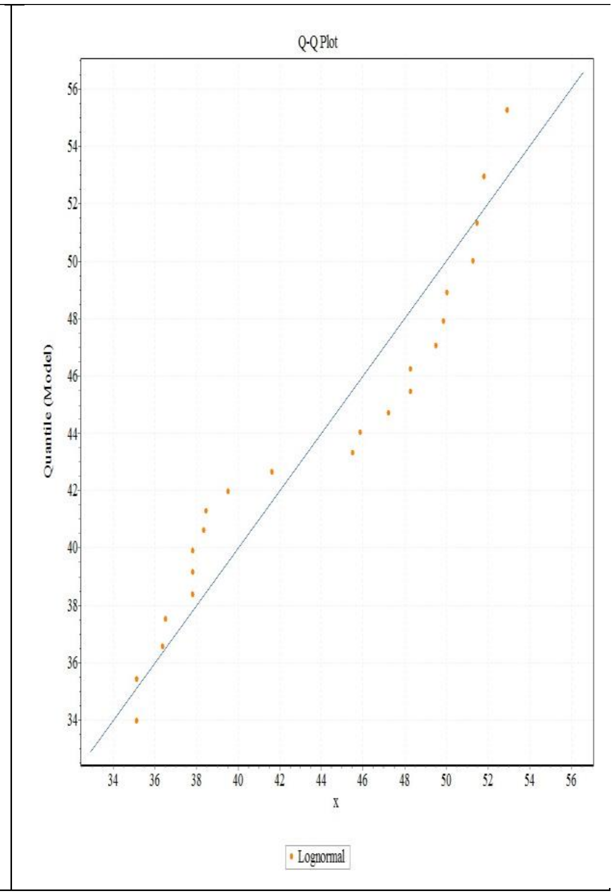
Q-Q Plot
Quantile (Model)
x
Lognormal

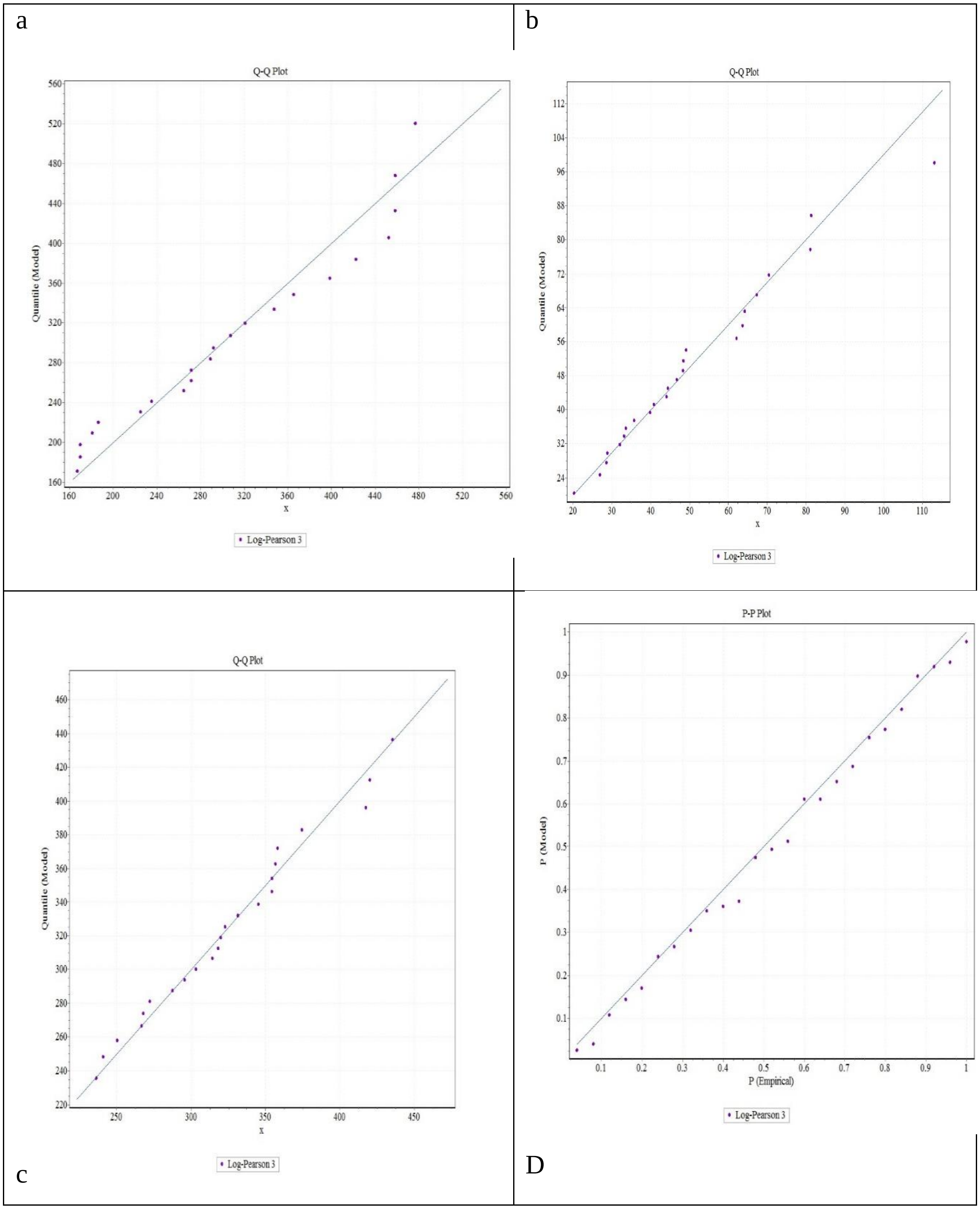
a
b
c
D
Q-Q Plot
Quantile (Model)
x
Log-Pearson 3
P-P Plot
P (Model)
P (Empirical)

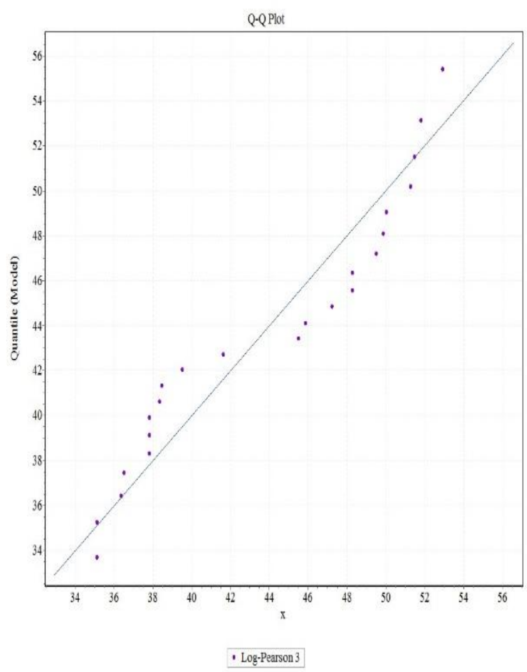
Q-Q Plot
Quantile (Model)
x
Log-Pearson 3

e

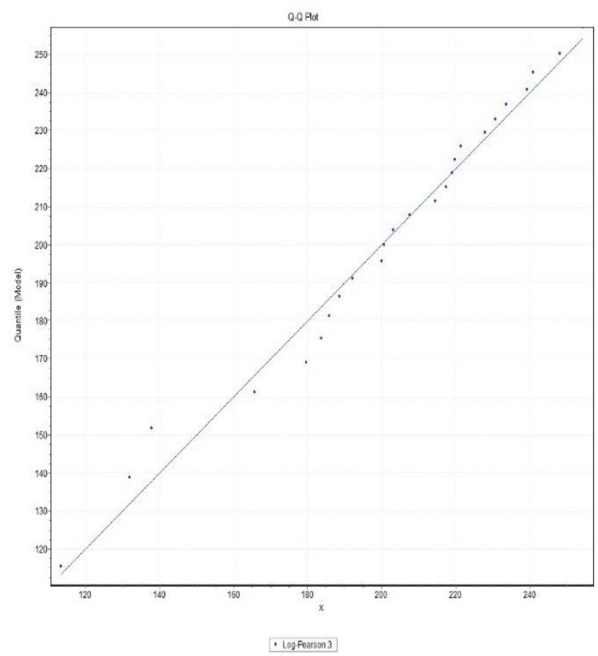
Q-Q Plot
Quantile (Model)
x
Log-Pearson 3

f